

2007

## Nonlinear analysis and active stiffness control of an air-mounted system

Pooya Mahmoudian  
*University of Dayton*

Follow this and additional works at: [https://ecommons.udayton.edu/graduate\\_theses](https://ecommons.udayton.edu/graduate_theses)

---

### Recommended Citation

Mahmoudian, Pooya, "Nonlinear analysis and active stiffness control of an air-mounted system" (2007).  
*Graduate Theses and Dissertations*. 4137.  
[https://ecommons.udayton.edu/graduate\\_theses/4137](https://ecommons.udayton.edu/graduate_theses/4137)

This Thesis is brought to you for free and open access by the Theses and Dissertations at eCommons. It has been accepted for inclusion in Graduate Theses and Dissertations by an authorized administrator of eCommons. For more information, please contact [mschlangen1@udayton.edu](mailto:mschlangen1@udayton.edu), [ecommons@udayton.edu](mailto:ecommons@udayton.edu).

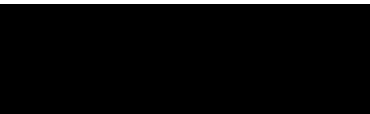
# **NONLINEAR ANALYSIS AND ACTIVE STIFFNESS CONTROL OF AN AIR-MOUNTED SYSTEM**

Thesis  
Submitted to  
The School of Engineering  
University of Dayton

In partial fulfillment of the requirement for  
the degree  
Master of Science in Mechanical Engineering  
by  
Pooya Mahmoudian  
Dayton, Ohio  
December, 2007

NONLINEAR ANALYSIS AND ACTIVE STIFFNESS CONTROL OF AN AIR-  
MOUNTED SYSTEM

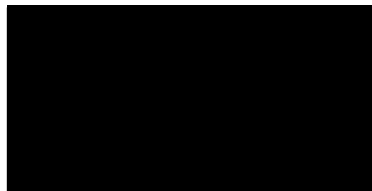
APPROVED BY:




Reza A. Kashani, Ph.D  
Advisory Committee Chairman  
Professor, Mechanical and  
Aerospace Engineering Department



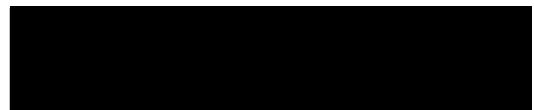
Robert A. Brockman, Ph.D  
Committee Member  
Professor, Civil and  
Environmental Engineering  
Department



Michael L. Turner, Ph.D  
Committee member  
Assistant Professor, Mechanical and  
Aerospace Engineering Department



Malcolm W. Daniels, PhD  
Associate Dean  
School of Engineering



Joseph E. Saliba, Ph.D, P.E.  
Dean, School of Engineering

## **ABSTRACT**

### **NONLINEAR ANALYSIS AND ACTIVE STIFFNESS CONTROL OF AN AIR-MOUNTED SYSTEM**

Name: Mahmoudian, Pooya  
University of Dayton  
Advisor: Dr A.R Kashani

Many undesirable vibrations are accompanying us in everyday life. Purpose of isolation is to minimize vibration transmission to the object of isolation from the mounting base or vice versa. Contrary to passive isolators (elastomeric or metallic), active isolators are adaptable to different dynamic scenarios. They usually consist of at least one adjustable isolator connected under the command of an active controller.

This thesis introduces a novel active and semi-active air suspension system. Each consists of an air spring as its adjustable isolator and an active or semi-active controller which controls the stiffness and damping of the air isolation system.

The semi-active approach was based on the fact that a decrease in the volume of the enclosed air inside of an air spring results in an increase in stiffness. Validity of this approach was verified using finite element analysis of an air-mounted system and showed very good agreement with the expected analytical results.

In the active control approach, to control the stiffness, a servo-valve was used to let the air in or out of the air spring in response to the signal received

from a controller board. The control board used measurements of the acceleration and displacement of the isolation system along with the user defined values of stiffness and damping , desired by the user, to control the dynamics of the isolation system utilizing a feedback scheme.

The validity of the active control approach was initially checked by a computer simulation and later by a real 1-DOF air-mounted system in the lab. The results showed between 125% to 300% increase in stiffness for the specific set-up that was used.

## **ACKNOWLEDGEMENTS**

My special thanks to Dr Kashani, my advisor, for giving me the opportunity to work on this thesis, and for directing it with his patience and expertise.

I would like to express my appreciation to everyone who has helped me with the work. This includes Dr Brockman for his guidance on the finite element analysis part and Kathryn Wetzel for her kind help in correcting the text.

## **PREFACE**

Air isolation systems, due to their softness, are desirable for many isolation applications. The problem with soft isolation is the high amplitude of vibration when a shock input is applied to the system. Therefore, an ideal air isolation system's stiffness should be adaptable to different isolation scenarios. The research performed in this thesis is in response to the need for control the stiffness of air isolation systems using semi-active and active control strategies.

## TABLE OF CONTENTS

ChapterI .....	10
Introduction .....	10
I.1    Significance of stiffness control in vibration isolation.....	12
I.2    Air springs .....	13
I.2.1    Advantages of Air springs .....	14
I.2.2    Air spring types used in vibration isolation .....	15
I.3    Previous research on air suspension systems .....	18
ChapterII .....	22
Semi-active control approach.....	22
II.1    Simplified Model.....	24
II.1.1    Static analysis .....	26
II.1.2    Frequency analysis .....	27
II.1.3    Results .....	28
II.2    Main model (Pneumatic air spring).....	30
II.3    The semi-active approach.....	34
II.4    Results .....	35
ChapterIII .....	37
Active Control Approach .....	37
III.1    Velocity measurement.....	38
III.1.1    Direct displacement differentiation .....	40
III.1.2    Acceleration integration.....	41
III.1.3    Kinematic Kalman Filter .....	42
III.2    Analytical Approach .....	44
III.2.1    Valve Simulation .....	45
III.3    One Degree of Freedom (1-DOF) Air-mounted System Simulation .....	53
III.3.1    Results .....	54
III.4    Active Control Scheme.....	55
III.4.1    Results .....	56
ChapterIV .....	58
Summery and Recommendations .....	59
ChapterV.....	61
Future works .....	61
References.....	62



## LIST OF FIGURES

Figure 1-1 Transmissibility diagram of a simple second order system .....	12
Figure 1-2 Bode diagram of a second order system (displacement/force) .....	13
Figure 1-3 Pneumatic air spring/mount .....	16
Figure 1-4 Convolute air spring .....	17
Figure 2-1 Axisymmetric view of a pneumatic air spring .....	24
Figure 2-2 Sketch of an air simple cylinder-piston system .....	24
Figure 2-3 Two-dimensional sketch of the simplified finite element model .....	27
Figure 2-4 Mode shapes of the initial model .....	30
Figure 2-5 Final partitioning of the pneumatic air spring model .....	33
Figure 2-6 Border of tied surfaces are marked by magenta color .....	33
Figure 2-7 Final mesh .....	34
Figure 3-1 Simple second order system resembling a spring, mass, and dashpot .....	38
Figure 3-2 An alternative block diagram of a 2nd order system .....	38
Figure 3-3 change of pressure versus time for linear change in flow. ....	40
Figure 3-4 Block diagram of a second order system with a displacement differentiation .....	41
Figure 3-5 Time response of an AC coupler versus a pure integrator .....	41
Figure 3-6 Frequency response of an AC coupler versus a pure integrator .....	42
Figure 3-7 Block diagram of a kinematic Kalman estimator. ....	43
Figure 3-8 Experimental frequency response of the valve for input voltage of 1 (vppk) for different mount pressures .....	46
Figure 3-9 Experimental frequency response of the valve for input voltage of 2 (vppk) for different mount pressures .....	47
Figure 3-10 Experimental frequency response of the valve for input voltage of 3 (vppk) for different mount pressures .....	47
Figure 3-11 Experimental frequency response versus analytical response (blue thick line) of the valve for input voltage of 1 (vppk) and different mount pressures .....	49
Figure 3-12 - Experimental frequency response versus analytical response (blue thick line) of the valve for input voltage of 2 (vppk) and different mount pressures .....	50
Figure 3-13 - Experimental frequency response versus analytical response (blue thick line) of the valve for input voltage of 3 (vppk) and different mount pressures .....	50
Figure 3-14 Output pressure change of the valve for input voltage of 1 (vppk) and frequency of 1 (Hz) .....	52
Figure 3-15 Servo-valve simulation .....	52

Figure 3-16 1-DOF air-mounted system simulation.....	54
Figure 3-17 Time response of the system to a shock input with different velocity feedbacks.....	55
Figure 3-18 The active control scheme.....	57
Figure 3-19 FRF of the air-mounted system with a pneumatic air spring .....	57
Figure 3-20 FRF of the air-mounted system with a convoluted air spring .....	58

## **Chapter I**

### **Introduction**

Many undesirable vibrations are accompanying us in everyday life. Cars, motors, machine tools, buildings and industrial plants are just a few examples where such vibrations are experienced. Sensitive equipment like optical tables should be isolated from any source of vibration that can affect their functionality. The purpose of isolation is to minimize vibration transmission to the object of isolation from the mounting base or vice versa. In other words, dynamic coupling between the vibration source and the isolated object should be weakened. Most isolated structures can be simplified as a spring and dashpot attached to a mass (representing the object of isolation). Spring represents the stiffness and dashpot represents the damping of the isolation system. In this thesis, the name “dynamic properties” refers to the stiffness and damping of such a system. However, this separation of dynamic properties is not identical in real isolators. In fact, most isolators have one or more components that do the job of both stiffening and damping.

There are different methods of isolation discussed in the literature which can be categorized as passive, semi-active and active methods.

Passive isolators benefit from their dynamic and material properties to reach the appropriate level of isolation. Since passive isolators cannot adapt their dynamic properties to different shock/vibration inputs in real-time, most passive isolators are designed for limited applications and/or dynamic situations.

Unlike passive isolators, active isolators are adaptable to different dynamic scenarios. They usually consist of at least one adjustable isolator under the command of an active controller. The adjustable isolator can be any isolator in which the dynamic properties can be changed with an actuation device. Examples can be found among hydraulic and air isolators which are suitable for high and low frequency applications respectively. When connected to an active controller via a servo-valve, their dynamic properties can be adjusted by changing the pressure of the enclosed fluid.

Although active isolation systems are more elaborate and expensive than passive or semi-active types, they are preferred in the industry. In fact, since utilizing any isolator has its own side effects on the dynamics of the isolated object, an active isolator provides more options for the user to minimize these effects and better benefit from the dynamics of the isolation system.

This thesis introduces a novel active and semi-active air suspension system. Each consists of an air spring as its adjustable isolator and an active or semi-active controller which controls the stiffness and/or damping of the air isolation system. In the semi-active approach, a method to change the stiffness of an air-mounted system is proposed. This method is based on changing the volume of the enclosed air which results in changing the stiffness of the isolation system. In the active control approach, in order to control these parameters, a servo-valve has to let the air in or out of the air spring in response to the signal received from the controller. The controller receives measurements of displacement (height) and acceleration of the mass (isolated object) in addition to the desired stiffness and damping specified by the user. Using this information, a feedback control scheme in the controller decides on the magnitude and phase of the signal to be sent to the servo-valve in order to realize and maintain the user defined stiffness, damping and height of the system.

### **I.1. Significance of stiffness control in vibration isolation**

Stiffness control has always been an interesting topic for vibration isolation. Lowering the stiffness increases damping and lowers the resonance frequency in a linear system and results in a softer isolation. On the other hand when a system is subject to shock inputs, high stiffness is desirable. Figure 1 shows transmissibility diagram of a simple second order system.

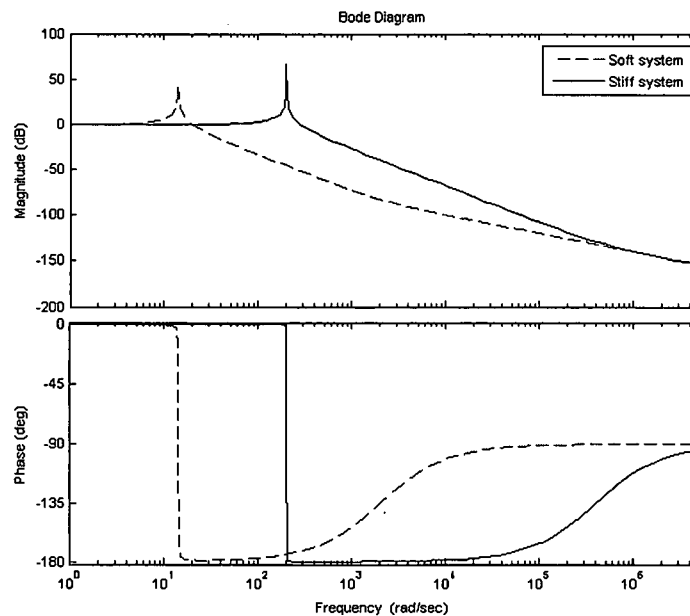


**Figure 1-1 Transmissibility diagram of a simple second order system**

As is shown in this figure, a soft isolation system transmits less force to the base or from the base to the subject of isolation. Therefore, having a soft isolator is always desirable in most isolation applications. On the other hand, for an isolation system that works at low frequencies (like an air-mounted system), the amplitude of vibration becomes high when a shock input is applied to the system. Figure 1-2 depicts frequency response of a soft and stiff isolation system.

Therefore, an ideal isolation system should become stiff when a shock is applied to the system and become soft when the system is not subject to any shock input to lessen the transmissibility.

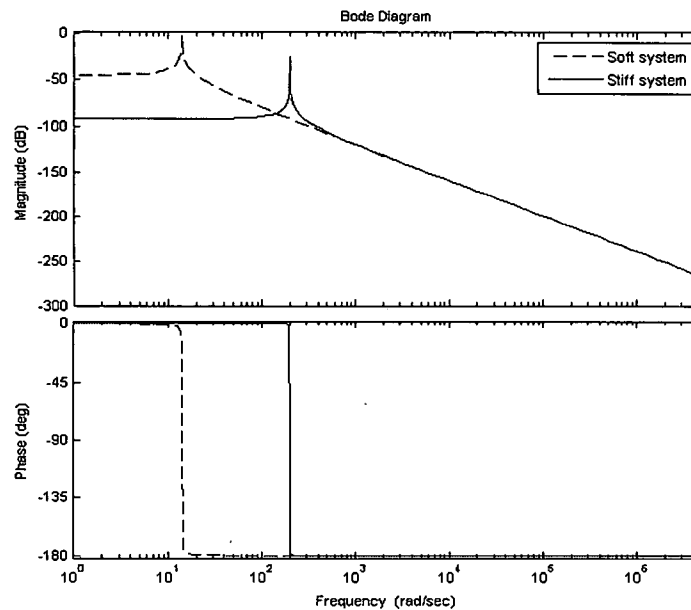


Figure 1-2 Bode diagram of a second order system (displacement/force)

## 1.2. Air springs

The adjustable isolator in this work is an air spring. Air springs use a contained volume of air inside an elastomeric bellows or sleeve to buffer cyclic motion, provide vibration isolation or serve as a pneumatic actuator. The adjustability character of an air spring is due to the fact that a change in pressure inside of the bellows can result in a change in the stiffness and damping. Moreover, this feature eliminates the need for installing different isolators on a system to accommodate both shock and vibration perturbations.

Feedback control theory is utilized in such isolators so that the controller can tune the dynamic properties of the isolator in response to the system's change in operating conditions. The outcome can be measured in the form of acceleration, pressure, displacement, etc.

#### I.2.1. Advantages of Air springs

1. Small operating height Air springs, due to their adjustable dynamic properties, can provide different stiffness values with a small variation in height. This feature makes air springs suitable isolators for applications where a compact installed height is desirable. Air spring heights are usually less than or equivalent to those of coil springs. Note that, despite theoretical possibility of designing a solid spring with a very low spring rate, it is usually not practical in reality because of the excessive static deflection of soft solid springs.
2. A spring with a wide load range Unlike solid springs that can have one constant spring rate; the spring rate of an air spring can be adjusted by changing its internal pressure. This unique capability gives the operator more freedom to use one suitable air spring size for a wide load range. A commercial pressure controller can also be utilized to maintain a constant pressure between air springs that are supporting a device to ensure that the isolated object is always level even when uneven loads are applied to the object.
3. Adjustable stiffness Adjustability of stiffness or spring rate depends on the internal air pressure, the change of the effective cross-sectional area, and air spring geometry. It means that the air spring can have almost a constant efficiency in a wide load range. This feature helps the designer to use the same air spring size to isolate an unevenly loaded object. The only side effect can be a small change in resonance frequency. A coil spring loses its

isolation effectiveness due to a very small change in the load. As mentioned before, a pressure or displacement control scheme (passive or active) can be utilized along with air springs to adjust their stiffness or internal pressure when any change in the applied load occurs.

4. Tunable natural frequency Depending on their type (pneumatic or convolution), air springs have high isolation capability. Resonance of a system with an air spring can be as low as one Hz. An additional auxiliary reservoir can even provide less stiffness and thus lower resonant frequencies. A static deflection of at least nine inches (which requires a large free length) is necessary to reach such a resonance frequency with a coil spring.

#### I.2.2. Air spring types used in vibration isolation

Pneumatic and convoluted air springs are the two main types of air springs currently used in most air suspension systems.

##### I.2.2.1. Pneumatic air springs

A *pneumatic* air spring is depicted in figure 1-3. This isolator does not have pneumatic damping (less than 2 percent material damping) can be counted for this device. The elastomeric body is made of neoprene and can contain a pressurized fluid like air. This isolator is designed in a way that the device is flexible in the vertical direction [2]. The elastomeric body also serves to cushion and limit motion in case of high vibration/shock inputs. Having an elastomeric body simplifies the mounting, especially in case of heavy equipment. When the spring is not inflated or under inflated due to shortage of pressurized fluid supply or a leakage, the object on the top can safely rest on this elastomeric body temporarily. Dale W. Schubert in [1] claims that this device has equal lateral and vertical stiffness. Thus, in case of an unpredicted shock/vibration input to the system in the lateral



direction, this air spring can provide the same springiness as in the vertical direction.

A pneumatic isolator is designed to provide a natural frequency of 3 Hz at 20 Psi, 6 Hz at 80 Psi, and almost 10 Hz when it is not inflated. These resonance frequencies highly depend on the mounted object as well [9].

Three rings on the side walls prevent the device from bulging on the sides to provide more vertical deflection and maintain enough stability in the lateral direction when the air spring is inflated. This air spring is manufactured in eight different sizes and can keep maximum of 80 Psi pressure inside and hold loads up to 19200 lbs. It should be noted that the presence of the steel rings maintains the internal cross-sectional area when the internal pressure changes.

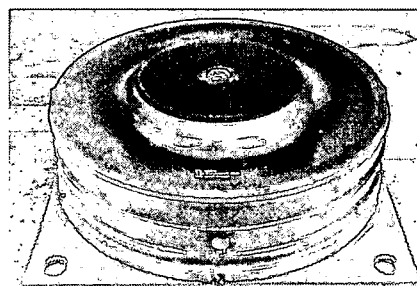
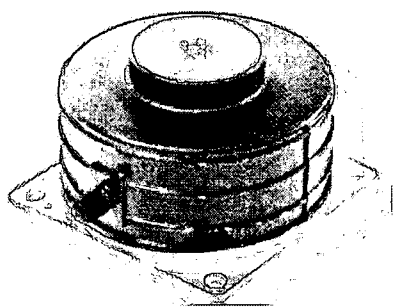


Figure 1-3 Pneumatic air spring/mount

#### 1.2.2.2. Convoluted air springs

Another type of air springs is the "*Convoluted*" type which is designed as bladders with a fabric reinforced elastomeric body. Figure 1-4 illustrates such an isolator. The reinforced rubber is attached to two circular plates on the top and bottom. Pressurized air goes into the isolator through an inlet and inflates it in the lateral as well as the vertical directions. Design of the reinforced rubber helps to minimize bulging on the sides. Having a very flexible elastomeric body provides larger working height, which is almost four times more than of the pneumatic type.

Geometry of this isolator can provide a very good stiffness in the vertical direction but it has almost no stiffness in the lateral direction. A remedy to this instability is to use additional constraints (like other air springs) for each unstable direction.

The cross-sectional area changes in a nonlinear manner up to about 20 percent due to the pressure and height of the spring. The effective volume  $v(x)$  of such an air spring can be approximated by the following formula [2]:

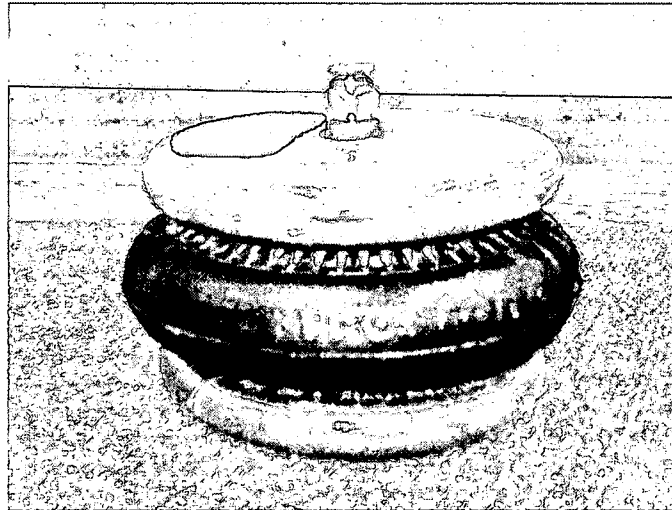


**Figure 1-4 Convoluted air spring**

$$v(x) = v_0 + v_1 \cdot x + v_2 \cdot x^2 \quad (\text{Eq1-2})$$

the effective cross-sectional area  $s(x)$  of this air spring can be expressed as:

$$s(x) = s_0 + s_1 \cdot x + s_2 \cdot x^2 \quad (\text{Eq 1-3})$$

where the air spring compression is for positive  $x$  and dilatation for negative  $x$ . Other symbols in the above equations denote the properties of a particular spring which should be determined experimentally. Furthermore, Agnew [4] investigated the approximate forms of convoluted air spring shells. In his technical note, he suggested two shell forms

consisting of circular arcs. The equations he presented are of great importance to calculate the first moment of inertia of the shell if necessary.

### **I.3. Previous research on air suspension systems**

The first and most common limitation in using air spring isolators is the lack of damping. An air-mounted system vibrates excessively when perturbed at its resonant frequency; moreover, because of the air spring's softness, the amplitude of the vibration becomes very high. This kind of perturbation, which can result in serious damages to the whole system, must be avoided. Therefore, previous research on air-mounted systems is mostly concerned with the damping issue. On the other hand, research on stiffness control of such systems has not been exclusively studied up to the time of this research and to the information of the author.

Hostens, Deprez and Ramon [3] investigated many passive and semi-active air suspension systems in which different control strategies were utilized. The first investigation was done solely on air springs. The benefit of using air springs rather than conventional spring-dashpot systems was found to be the following:

- Inherent damping because of the compressibility of the air.
- Better protection against end-stop limits of the system due to higher increase in stiffness at end-stops.

The use of an extra air volume to lower the resonance frequency was investigated next. The results showed that such an auxiliary air reservoir affected dynamic properties of the air spring without changing its operational height, which is of great importance. The last part of their research was done by connecting a throttle valve to the air spring. As a

result, a large amount of air passed through the throttle valve at a slow rate at low frequencies, and when the operating frequency increased the same amount of air passed through the valve with much higher speed which resulted in a very high damping. Damping increased until the valve blocked and resulted in a pure spring with almost no damping. This effect was also beneficial to the vibration attenuation because it completely eliminated the Coulomb friction generated by the suspension system. None of these systems allow configurable control of damping and/or stiffness; therefore, the resulting suspension system can only be effective at a certain frequency range with variable damping and stiffness at different applied loads.

Luque and Mantaras [7] presented simplified models for pneumatic suspension systems in semi-trailers. They proposed a semi-active height control scheme to maintain the height of a trailer against the pressure change. According to their investigation on the characteristic curves of a pneumatic air spring, the relationship between the applied load on the air spring and its height was almost linear in a certain range of load and height. This assumption simplified their calculations of the damping and stiffness of the system to a simple second order dynamic system.

Stein and Ballo [5] worked on active control systems for the driver's seat for off-road vehicles. Their control scheme was based on the compensation principle acting on an electro-hydraulic suspension system. They showed that "even with a slow hydraulic proportional servo-system which is controlled by analogue electronics connected in series with a conventional spring-damper passive vibration control system of the standard driver's seat, a three-fold improvement in overall vertical vibration influence on the sitting earth moving machine driver can be reached." Stein [6] suggested a proportional pressure control scheme to lower the controllability burden on the controller. In each of their proposed systems ([5] and [6]), an air spring was used along with a hydraulic

actuator (to add damping to the system) and/or a parallel leaf spring (to maintain the initial height).

The active control systems described above give the user an option to change the resonance frequency of the system, but they can not separate controllability of stiffness from damping. Hence, a change in any of these two properties results in an unavoidable change in the other one. The proposed active air suspension system in this thesis utilizes a control scheme which provides on-demand configurable stiffness and damping control on the system. Such a novel suspension system is ideal for vibration isolation of sensitive machinery and electronics where the change in stiffness and damping should be considered carefully for the best isolation outcome. Unlike Stein's and Ballo's, this suspension system does not require parallel passive isolators (hydraulic or metallic) to enhance its overall performance. The control scheme in this system only takes advantage of the adjustability character of air springs in order to control the damping and stiffness, both on-demand and separately.

In Chapter II a finite element analysis of a pneumatic air spring was conducted to gain insight into the dynamic properties of a simple one-degree-of-freedom (1-DOF) air-mounted system. Finally, a semi-active stiffness control strategy was introduced and implemented in the finite element model. The semi-active approach based on changing the enclosed air's volume was tested on the model. The results in comparison with an analytical solution indicated the validity of the semi-active approach.

Chapter III describes an active approach to stiffness control of air-mounted systems. As mentioned before, both suggested active and semi-active control strategies take advantage of adjustability of air springs. In the active case, response of the system was measured with an accelerometer and an ultra sonic displacement sensor. Velocity was estimated using these measurements with a kinematic Kalman filter [8].

The active controller was based on feeding a damping and stiffness control force back to the isolator via a servo-valve. To validate the active control strategy the simulation of a 1-DOF air-mounted system was performed. This simulation included the servo-valve and the air spring along with the necessary feedback control loops. To simulate the servo-valve performance, its experimental transfer function and the transport delay of the servo-valve and the control board were determined. The effect of the active control strategy on stiffness was tested and showed 200 percent increase in the stiffness of the specific set-up used for the simulation.

Despite commonly used active controllers for air-mounted systems, the proposed controller does not require any additional actuator to overcome any damping or stiffness issue. In fact, any parallel actuator is replaced by a high-speed servo-valve which can be installed anywhere between the air supply and the air spring. Furthermore, using such a servo-valve does not affect the cost of the isolation system very much. In many applications passive air isolators are being commonly used along with regular control valves that maintain their internal pressure with a height or pressure controller. To use the proposed isolation system in these vehicles, one needs to change the control valve to a servo-valve. Accordingly, the only additional cost is the price difference between a regular control valve and a high-speed servo-valve.

The fifth Chapter represents the summary of the work with recommendations and Chapter VI is about the future works.

## **Chapter II**

### **Semi-active control approach**

One reason, amongst many others, for choosing air isolation is *adjustability*; one of the attributes (mainly stiffness and/or damping) of air springs can be readily modified by variety of means. These means include further inflation/deflation, timing of this inflation/deflation, change of the internal medium, etc. Proper exploitation of this adjustability is crucial in realizing any successful actively or semi-actively controlled air suspension system. This, in turn, necessitates the exploration of the mechanics of air springs.

Such exploitation requires thorough understanding of the nonlinear behavior of air springs. Sources of nonlinearity are:

- a) The material (either rubber or rubber and fabric composite) making up the bellows.
- b) Change in geometry (more specifically the effective cross-sectional area).

Hence, complexity of the air spring/mount mechanics makes the use of finite element method in modeling it a must.

ABAQUS finite element analysis (FEA) software has been used in a step by step approach to modeling a typical air-mounted system. Such a system usually consists of an air spring with a mounted mass on its top. First, a FEA model of simple geometry, which has an analytical solution, was analyzed. This simplified model helped exploring the ABAQUS software features required to model the air spring. After gaining

experience with the finite element analysis of the simple model, analysis of a commercially available pneumatic air spring was begun. With the model developed and its linear behavior verified with analytical results, nonlinear static and dynamic analyses were performed.

As in the simplified model, air, the rubber bellow, and reinforcing steel rings (built into the rubber bellow) with their corresponding linear and nonlinear material properties were all modeled. The Mooney-Rivlin hyperelastic material model and uniaxial stress-strain test data, provided by the manufacturer, were used to model the nonlinear behavior of the neoprene making up the bellow. Air was modeled using quadratic linear acoustic elements and rubber was modeled using quadratic axisymmetric stress elements. Coupling between acoustic and structural elements was implemented in the model using the "Tie" feature in ABAQUS. Partitioning was performed to have the best possible match between nodes on the tied surfaces. The linearized model was validated by the limited experimental data available, indicating a good agreement. Discrepancies between the FEA results and experiment are attributed to inadequate material model data.

The main idea of the semi-active approach is to create an air suspension system which does not necessitate constant real-time control on its stiffness. The method proposed to accomplish this goal is to use an incompressible fluid, i.e. water, beside a compressible medium, i.e. air, in air springs. The described semi-active strategy was verified for a pneumatic air spring with finite element analysis method



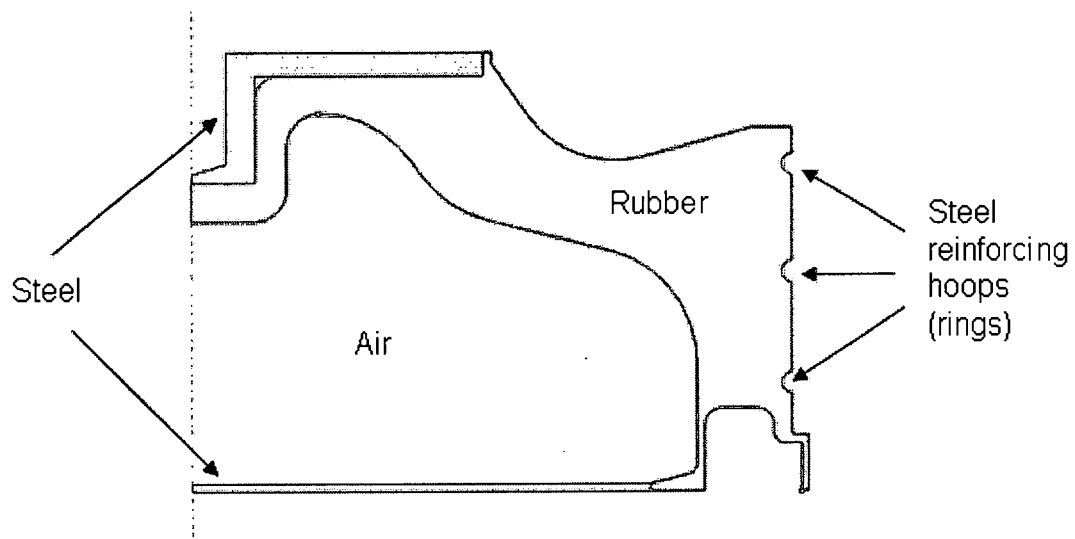


Figure 2-1 Axisymmetric view of a pneumatic air spring

### II.1. Simplified Model

As mentioned before, the simplified model was a cylinder with air inside as depicted in figure 2-1. The weight of the mass on the top increases the internal air pressure that leads to a rise in the air bulk modulus and density. The springiness of the system is provided only by the inverse of air compliance.

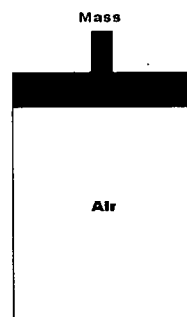


Figure 2-2 Sketch of an air simple cylinder-piston system

Assuming a constant speed of sound for air in most air springs' operational range of pressure (usually between 20 to 80 Psi), the bulk modulus can be determined using the relationship below:

$$C_{com} = \frac{V}{\rho c^2} \quad \text{Eq 2-1}$$

where  $C_{com}$  is the air compliance,  $V$  is the cylinder internal volume (or air volume),  $c$  is the speed of sound,  $\rho$  is the air density at the internal pressure. The relationship between the pressure and density of air in the mentioned pressure range can be considered linear and of the form:

$$\rho = \rho_0 P \quad \text{Eq 2-2}$$

in which  $\rho_0$  is the corresponding air density at the pressure of  $P$  in atmospheric unit and  $\rho$  is the air density at one atmosphere (approximately  $1.2 \text{ kg/m}^3$ ). Furthermore, stiffness of such a cylinder can be found by:

$$K_{equal} = \frac{A^2}{C_{com}} \quad \text{Eq 2-3}$$

where  $A$  is the effective cross-sectional area of the cylinder and  $K_{equal}$  is the equivalent stiffness of the system (provided exclusively by the internal air).

With the amount of mechanical stiffness and mass along with the assumption of having a very low damping ratio, resonance frequency can be calculated by:

$$\omega = \sqrt{\frac{k_{equal}}{m}} \quad \text{Eq 2-4}$$

in which  $\omega$  is the system resonance frequency and  $K_{equal}$  is the air compliance and  $m$  is the mounted mass on the isolator.<sup>1</sup>In fact, by the

---

<sup>1</sup> Since in air springs the damping ratio is very low (about two percent), one can calculate the damping coefficient after determining the equivalent stiffness and the resonance frequency:  $B = 2\zeta\sqrt{K_{equal}m}$

$B$ = Damping coefficient (Dashpot damping constant)

$\zeta$  =Damping ratio

mentioned assumptions, properties of the cylinder in Figure 1 are translated to an identical spring-mass-dashpot system.

Figure 2-1 shows an axi-symmetric sketch of a pneumatic air spring as the main model. Considering the shape of this air spring, the simplified model was created (see figure 2-3). As shown in figure 2-3, a thin diaphragm connects the circular top plate to the cylinder. Load (mass) is mounted on top of this circular plate. All parts of the model except the diaphragm are made of solid elements with extremely high modulus of elasticity. The diaphragm has a very low modulus of elasticity to offer enough flexibility to allow the top circular plate move up or down freely. Such a model resembles the simple cylinder in figure 2-2. Therefore, all former relationships and formulas to determine dynamic properties of the cylinder apply to this model with a negligible error.

#### II.1.1. Static analysis

Total stiffness of the model is sum of the structural stiffness (provided mainly by the diaphragm) and the equivalent stiffness of air (which is proportional to the air compliance).

$$K_{total} = K_{diaphragm} + K_{air-equivalent} \quad \text{Eq 2-5}$$

The goal of the static analysis is to minimize the structural stiffness of the model so that the stiffness is mainly provided by the air so that the stiffness becomes predictable by Eq 2-3. The structural stiffness comes from the diaphragm which is the only flexible part of the structure. Minimizing this stiffness reduces the overall stiffness to that of the air, which makes this model similar to the rigid cylinder in figure 2-2.

Having minimized the structural stiffness, the spring constant is proportional to the compliance of the internal air (see Eq 2-3). Note that since all parts are rigid and the acoustic medium (air) is not flowing in or out of the model, the damping ratio is very small (about two percent). Therefore, dividing the applied load on the top circular plate by the

maximum deflection (extracted from the result of the static analysis) gives the total stiffness at that each specific pressure and height.

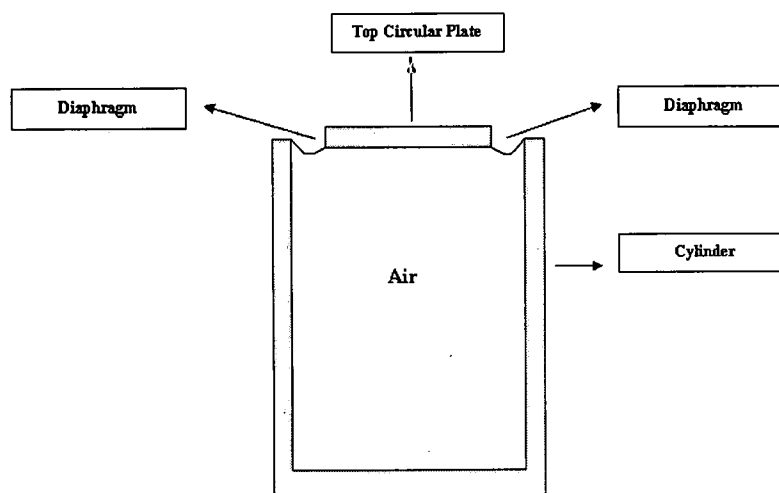


**Figure 2-3 Two-dimensional sketch of the simplified finite element model**

This stiffness from the static analysis had very good agreement with the analytical calculations described previously (using formulas Eq 2-1 to Eq 2-5). Table 2-1 shows the results from the finite element analysis and the analytical solution. Note that although the acoustic elements were included in the model, ABAQUS static solver neglects them due to their lack of displacement degrees of freedom.

**Table 2-1**

	Analytical Solution	Finite Element Analysis
Resonance (Hz)	1.91	1.84
Total Stiffness(N/m)	22430	20100

### II.1.1.2. Frequency analysis

The static analysis was followed by a frequency analysis to extract the resonance of the model. These results were validated later through experimentation (see table 2-1). Acoustic elements were coupled with the

structural solid elements using “Tie” feature in ABAQUS. This command basically ties the nodes on the surfaces to be coupled by relating the pressure degrees of freedom in the acoustic elements to accelerations in the solid elements. Despite the former static analysis, acoustic elements were taken into account by the frequency solver. The first natural frequency is shown in table2-1 which has very good agreement with the analytical solution.

The simplified model gave an insight to the properties of the final model and the features that must be used in the analysis.

### II.1.3. Results

Figure 2-4 shows the frequency solver results. The first mode (with very low natural frequencies) is a miscellaneous mode. Modes 3 and 4 are also structural modes that are related to the diaphragm, and mode 2 is the first Structural mode.

Since the third mode shape shows almost zero pressure change from the bottom to the top of the cylinder, it can be inferred that this mode is the first structural mode.

#### 1. First structural mode

With 272 kilograms mass on the top and 2 atmospheric internal pressure, the first natural frequency was found to be 1.98 Hz.

#### 2. First acoustic mode

The first acoustic mode can be circumferential or axial depending on its associated wave length. Each wave length in return depends on the diameter or height of the cylinder. The bigger the wave length, the smaller its natural frequency is.

*Acoustic wavelength (m)*

*c= Speed of sound (m/s)*

*n= c/      Natural frequency (Hz)*

For axial acoustic mode the wave length is twice the cylinder height.

Thus,

$$\lambda = 0.18 \times 2 = 0.36(\text{meters})$$

And furthermore,

$$\omega_n = 955.55(\text{Hz})$$

For circumferential acoustic mode the wave length is approximately twice the cylinder radius, thus:

$$\lambda = 0.19 \times 2 = 0.38(\text{meters})$$

And the resonance frequency is:

$$\omega_n = 451.31(\text{Hz})$$

Considering the mode's frequencies, the circumferential acoustic mode is mode three with the resonance frequency of 427.5 Hz and the first axial acoustic mode is mode five with the resonance frequency of 949.39 Hz. However, since the model includes the structural elements as well, these modes are not purely acoustic. But close agreement of the calculation above with the results from the finite element model is another proof that the model properties were close to what was expected.

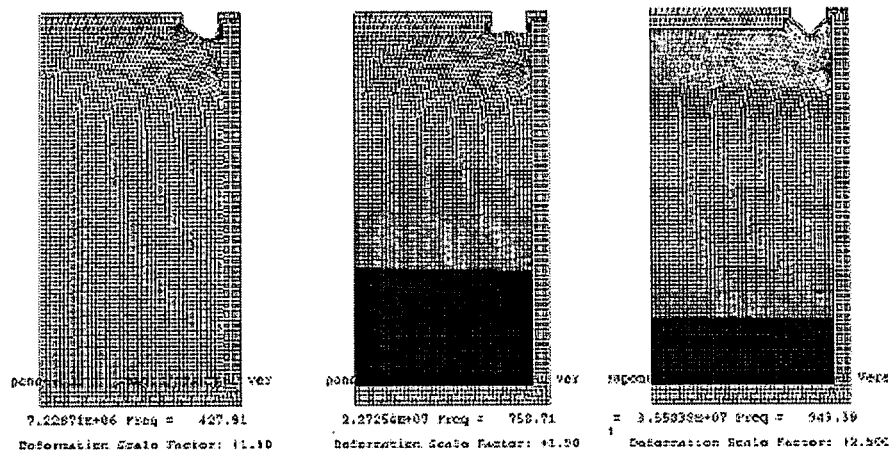
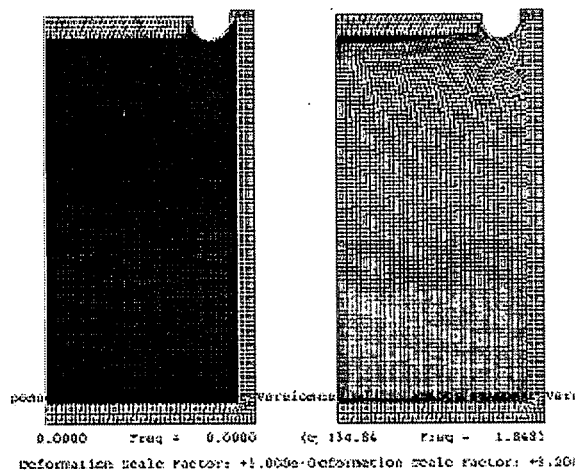


Figure 2-4 Mode shapes of the initial model

## II.2. Main model (Pneumatic air spring)

Figure 2-1 shows a two-dimensional view of a pneumatic air spring as the main model. A large portion of the air spring is made of rubber. The top circular plate is where the mass or object of isolation should be mounted, and the bottom circular plate should be mounted on the base.

The steel reinforcing hoops help maximize the height of the air spring by preventing it from bulging on the sides. For this application, since only the first resonance frequency was of interest, these hoops were replaced by constraints to block lateral motion. Note that replacing the

reinforcing hoops with constraints eliminates some modes that are not axis-symmetric at high frequencies.

Air was modeled using quadratic linear acoustic elements, and the rubber bellows was modeled using quadratic linear axis-symmetric stress elements with hybrid (mixed) formulation. In addition, the steel parts were modeled with quadratic linear axis-symmetric elements enhanced with incompatible modes formulation.

In ABAQUS/Standard, the use of "hybrid" (mixed formulation) elements is recommended in both incompressible and almost incompressible materials. This formulation eliminates special volumetric treatment (which does not affect such materials) and therefore saves the amount of computations.

In fact, if fully or selectively reduced-integration displacement elements are used with hyperelastic materials (which are almost incompressible) a penalty method is used to include the constraints which impose the incompressibility. This penalty method may result in numerical difficulties during the analysis; therefore, the hybrid formulation elements (which are selectively reduced-integrated as well) are suggested for use with hyperelastic materials. The only disadvantage might be a slightly more expensive calculation than analysis with regular displacement-based element types.

In addition to the displacement degrees of freedom, incompatible deformation modes are added internally to the structural elements for steel parts. The primary effect of these degrees of freedom is to eliminate the so-called parasitic shear stresses that are observed in regular displacement elements when they are loaded in bending. In other words, incompatible deformation modes remedy the stiffening due to Poisson's effect in bending. In regular displacement elements, there is always a linear variation of the stress in the vertical direction to bending in addition to the axial stress variation. This variation results in overestimation of the



stiffness, which can be prevented by utilizing incompatible deformation modes as described above.

Tie constraints in ABAQUS are used to tie two surfaces with the same or different element types during the simulation. Therefore, this feature can be used only with surface-based constraints definitions. In general, applications can be found in mechanical, coupled temperature-displacement, acoustic pressure, coupled acoustic pressure-displacement, coupled pore pressure-displacement, coupled thermal-electrical, or heat transfer simulations. To tie two surfaces together, first a slave and a master surface should be specified. It should be noted that each slave surface node should have the same motion, temperature, pore pressure, acoustic pressure, and electrical potential as of the node on the master surface to which it is closest. As mentioned before, although ABAQUS does not necessitate the nodes on both tied surfaces to be very closely matched in coordination, accurate results are sensitive to this issue. This task is attainable using partitioning<sup>2</sup>.

The "Partition" feature in ABAQUS divides a model into smaller parts without affecting the material, elements, couplings or analyses. It only affects the arrangement, size and flow of the elements according to its shape and the type and global size of the assigned elements. Figure2-5 shows the final partitions in the model[10].

---

<sup>2</sup> Note that since it is impossible to have a perfect node coupling between two tied surfaces, ABAQUS always gives maximum node adjustments in the \*.data file for user's records.

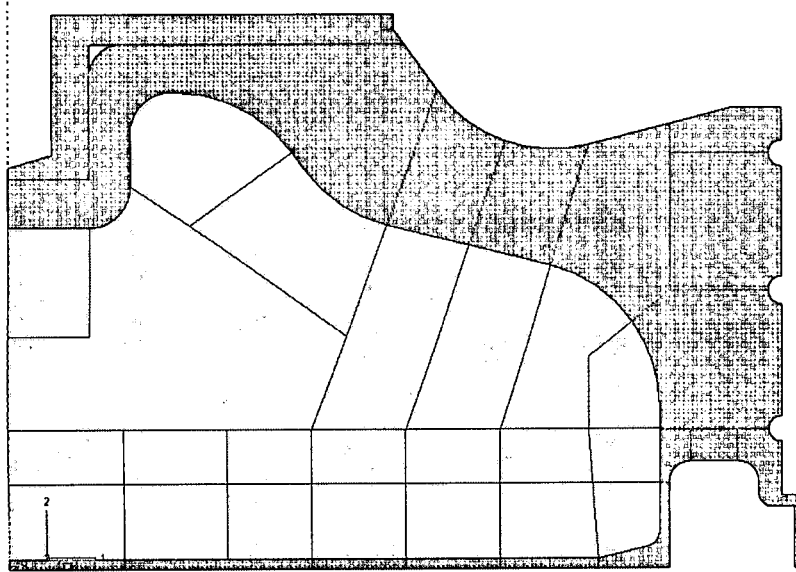


**Figure 2-5 Final partitioning of the pneumatic air spring model**

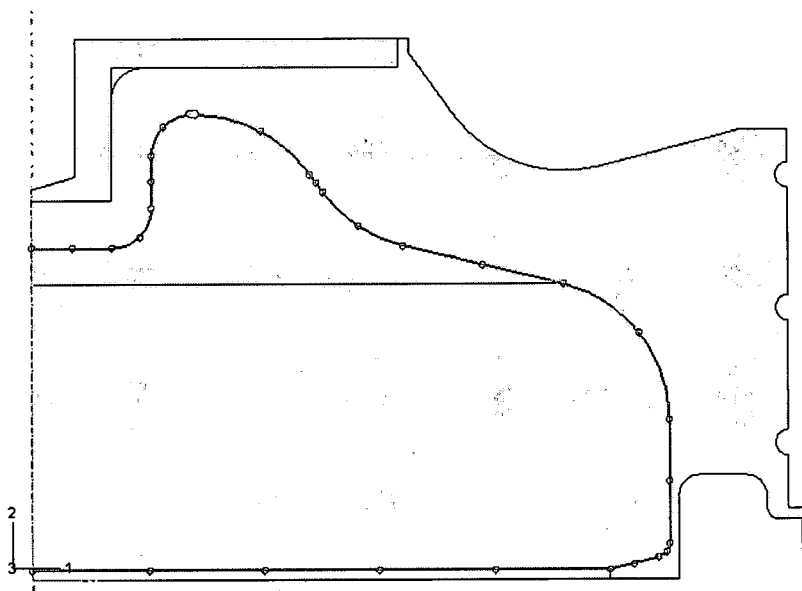


**Figure 2-6 Boarder of tied surfaces is the boarder of the air chamber and rubber bellows**

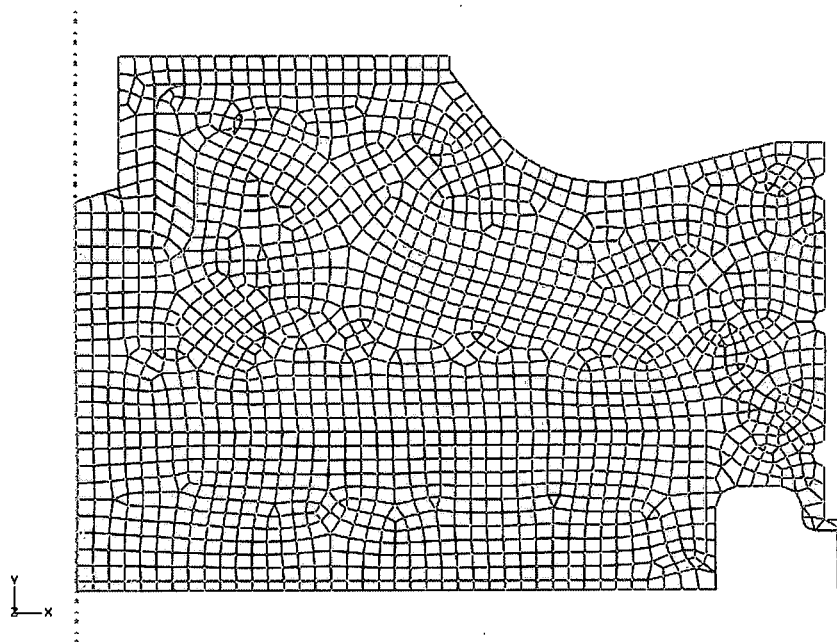


**Figure 2-7 Final mesh**

### **II.3. The semi-active approach**

Having validated the finite element model with experimental data (table 3-1), the semi-active approach was implemented. As previously described, the proposed method uses an additional medium besides air in the air spring in order to adjust its stiffness in a semi-active manner.

This control scheme is suitable for applications where change in stiffness is not required frequently. Therefore, when needed, a user can adjust the stiffness of the isolation system due to significant changes to the weight or arrangement of the loads' distribution of the mounted objects. Such a control strategy, together with commercially available pressure or height controllers for air-mounted systems, results in a very effective and rather inexpensive suspension system.

Stiffness in an air spring is inversely proportional to the compliance of its acoustic medium and/or of the incompressible fluid inside of it.

The relationship between the bulk modulus and density is of the form:

$$c = \sqrt{\frac{B}{\rho}} \quad \text{Eq 2-6}$$

where  $c$  is speed of sound,  $B$  is bulk modulus, and  $\rho$  is density of the acoustic medium. In this work water was used beside the air in order to increase the stiffness of the system. Main reasons for using water as the additional medium are that water:

- Has a density of about 1000 times more than air. Hence an increase in the density leads to an increase in the bulk modulus which directly increases the resonance frequency (see Eq2-6) and stiffness.
- Is incompressible. Therefore a change in the internal pressure does not affect its density.
- Does not react with rubber and rubber-like materials chemically.
- Is usually available and rather inexpensive in small amounts (Less than a gallon for a 6-DOF system with the largest commercially available air springs).

Since water stays in the bottom of the internal chamber and air stays on its top, these two mediums act like two springs in series which in general increases the stiffness more effectively than a parallel system of springs.

## **II.4. Results**

In the finite element model with 250 kg of mass on top of the air spring, the resonance frequency was found to be 5.98 Hz (37.573 rad/s). Considering Eq 2-5, the stiffness was calculated:

$$\omega \equiv \omega_n = \sqrt{\frac{K_{equal}}{m}} \quad K_{equal} \rightarrow \omega^2 m = 37.573^2 \times 250 = 3.5294 \times 10^5 \text{ N/m}$$

In another analysis, 1/5 of the air spring's internal volume was filled with water. The resonance frequency was found to be 6.66 Hz (41.84 rad/s). Using the same calculation above gave the equivalent stiffness of  $4.2777 \times 10^7 \text{ N/m}$ .

$$\text{Percent of the stiffness increase} = \frac{4.2777 \times 10^5 - 3.5294 \times 10^5}{3.5294 \times 10^5} \times 100 = 21.1\%$$

To verify this result another analysis was performed based on the change in internal air volume. When 1/5 of the volume was replaced by the water, the volume of the internal water decreases to 4/5 of the initial volume. Using Eq 2-1 shows that the new air compliance would be 20% less. Consequently, Eq 2-3 shows that the equivalent stiffness increases 20% as a result. This conclusion approved the stiffness increase determined by the result of the finite element model. Hence the semi-active control strategy should be considered valid.

In general, the stiffness change using the propose control strategy is not continuous. Thus, to have a continuous control on the stiffness a more elaborate active control scheme was studied in the next chapter.

## **Chapter III**

### **Active Control Approach**

In this chapter the active control approach is described. As discussed in Chapter 1, the dynamic properties of an air-mounted system can be modified by a number of means. One of these methods, imposing further inflation or deflation at the right time and the right magnitude, is the basis of this approach.

Note that in this thesis a special block diagram for a simple second order system is used. Figure 3-1 shows a regular second order system and Figure 3-2 shows the same system with an alternative block diagram. The advantage of this alternative block diagram is the simplicity in recognizing different forces acting on the system. For example in Figure 3-2 stiffness of the system is viewed as a spring force (proportional to displacement) fed back to the system with the gain of "k" equal to the spring constant.

In an air mounted system, stiffness is directly related to internal pressure. This stiffness can be modified if the change in pressure becomes controllable in a feedback control scheme. This scheme basically feeds a force back to the system that is proportional to displacement, i.e. a stiffness force. The overall stiffness can be modified if the feedback force is implemented at the right time with the right magnitude.

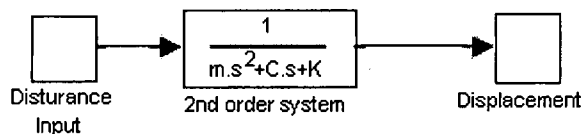


**Figure 3-1 Simple second order system resembling a spring, mass, and dashpot**

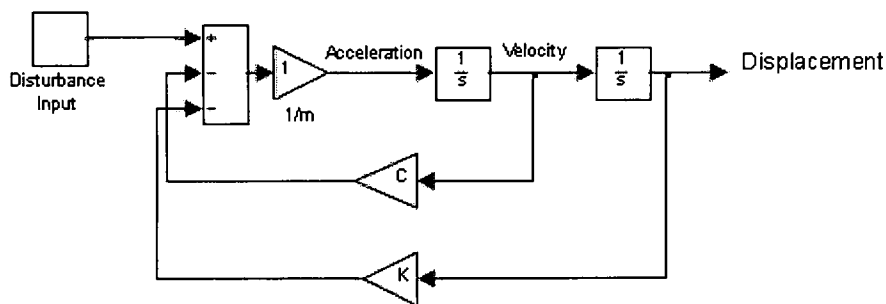


**Figure 3-2 An alternative block diagram of a 2nd order system**

The active control set-up consists of an air spring connected to a servo-valve. The servo-valve's spool position is controlled by a control board. One air exhaust and one air supply are connected to the servo-valve. The spool moves according to the signal being sent from the control board to the valve, which results in inflation or deflation of the air spring connected to the output of the valve.

The control board which resides inside a PC is where the control scheme is implemented. This board receives measurements of the acceleration and displacement of the mounted object and calculates the amount of voltage to be sent to the servo-valve. This voltage moves the spool from its central position to let some air in or out of the air spring.

### **III.1. Velocity measurement**

Having a negligible leakage in the system, an air spring acts like an integrator to the flow in the operating range of pressure (20 to 80 Psi). In

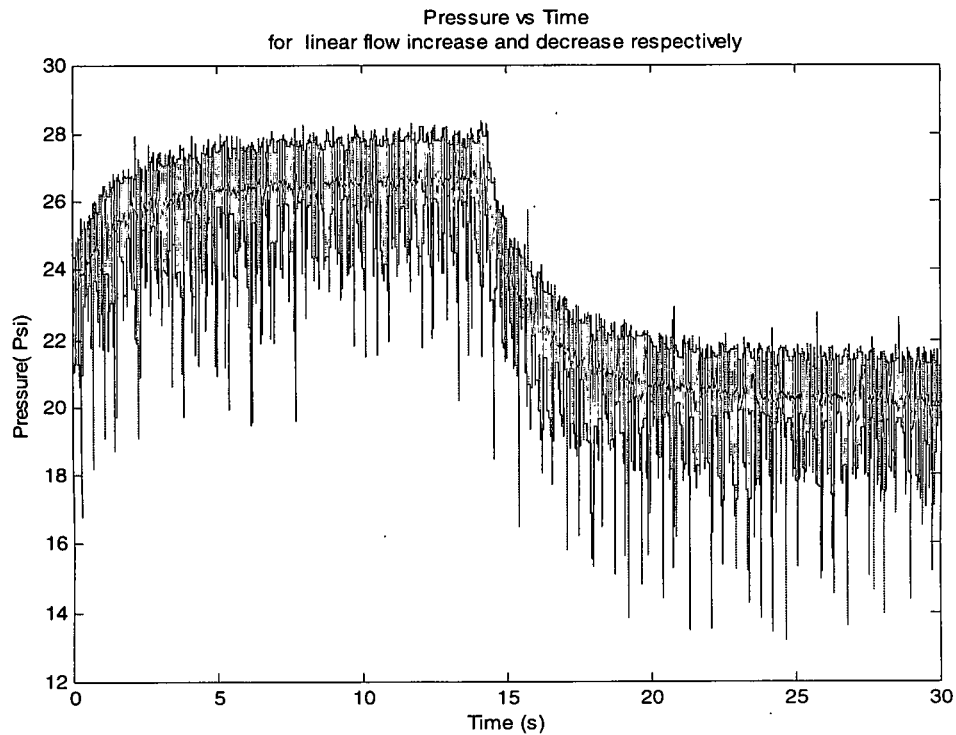
other words, an incoming flow to an air spring ends up increasing the internal pressure in proportion to the amount of air accumulated in the air spring.

Figure 3-3 depicts change in the air spring pressure in response to a step change in the voltage driving the spool, under constant supply air pressure. Considering that the bandwidth of the valve is by far larger than the bandwidth of an isolated mechanical system, the first order response of Figure 3-3, to a step change in valve opening (spool position) at a constant supply pressure, is an indication of pressure inside the air spring being the integral of flow in and out of the air spring.

This property indicates that to have a stiffness control force proportional to the displacement, a velocity feedback signal is required to be sent to the valve. As a result of the integration, discussed above, this force becomes proportional to the displacement which can affect the stiffness of the system. Considering the inconvenience of velocity measurement, we opted to estimate this velocity from the measurement of related readily measurable variables.

In this section, two major methods of determining/estimating velocity are described. These methods are acceleration integration and displacement differentiation each having their own advantages and disadvantages. Reasons for not using neither of these methods for the proposed active control scheme are described, and in the end, an alternative way of measuring the velocity, with a Kalman filter, is described.





**Figure 3-3 change of pressure versus time for linear change in flow.**

### III.1.1.1. Direct displacement differentiation

One way to determine velocity is direct displacement differentiation. A displacement measurement is always accompanied by high frequency noise; therefore, a second order low pass filter is required to remedy this noise issue. In the Laplace domain, the transfer function of such a filter is of the form:

$$T.F \text{ of a second order filter} = \frac{1}{s^2 + 2\zeta_f \omega_f s + \omega_f^2}$$

where,  $\zeta_f$  and  $\omega_f$  are the damping ratio and filter's corner frequency, respectively. The damping ratio of such filters are commonly taken as 1 (100%) and the corner frequency is set to at least 10 times higher than the resonant frequency of the system under study. The reason is to have the least phase change caused by the filter. Combined with a differentiator ("s")

in Laplace domain), the transfer function of the whole differentiator with a low-pass filter is of the form:

*Transfer function of the differentiator with a low pass*

$$filter = \frac{s}{s^2 + 2\zeta_f \omega_f s + \omega_f^2}$$

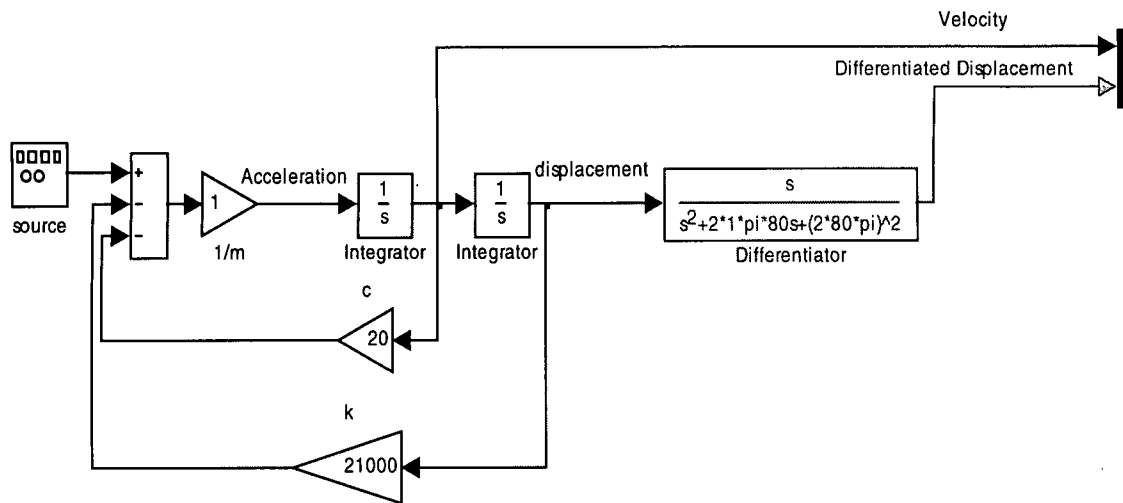


**Figure 3-4 Block diagram of a second order system with a displacement differentiation**

This method creates a phase lag in the resulting velocity signal which is not desirable for active control systems. In fact, the most important property of the velocity signal for our active control scheme is the phase. Further decrease in the corner frequency increases this phase lag even more. Increasing the corner frequency can remedy this issue but also results in letting a huge amount of noise into the system. Therefore, this method can not give a reliable velocity signal with an accurate phase.

### III.1.2. Acceleration integration

Another way to determine velocity is to integrate acceleration. All accelerometers have a certain amount of DC offset. This DC offset can be viewed as a constant value added to the measured acceleration. Considering that the integration of a constant results in a ramp function, this DC offset could saturate the velocity derived from acceleration integration. To overcome this problem, instead of using a pure integrator an AC coupler with a low corner frequency should be utilized. A typical AC coupler is a first order system. When combined with a low-pass filter, the transfer function of the whole system is of the

form:  $\frac{s}{s^2 + 2\xi\omega_n + \omega_n^2}$ , in which  $\omega_n$  is the AC coupler's resonant frequency which

should be greatly below the resonant frequency of the system under study to prevent the AC coupler from causing excessive phase distortion. Figure 3-6 compares the frequency response functions of a pure integrator and an AC coupler approximating it. Note that at high frequencies, i.e., the frequency range of interest, the AC coupler and pure integrator have the same frequency response functions.

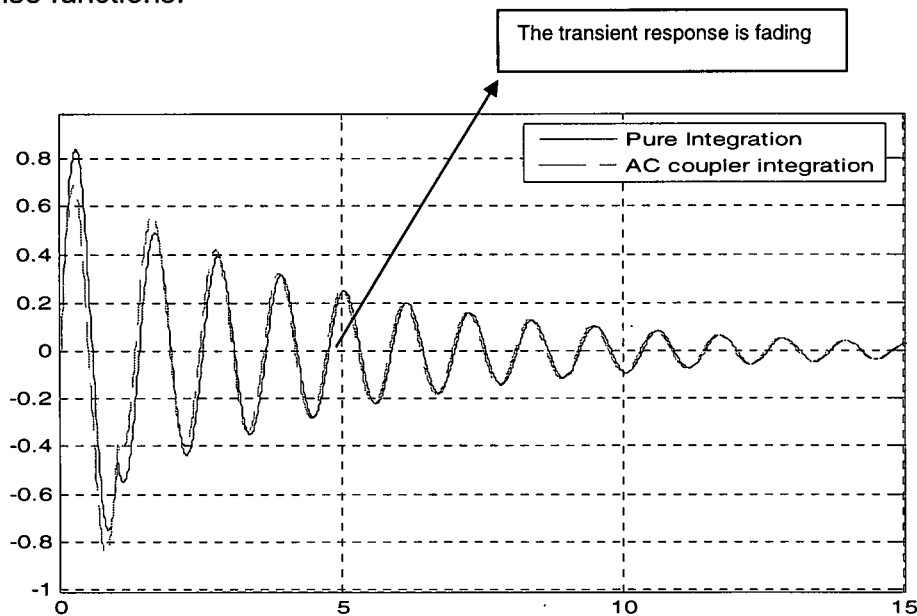
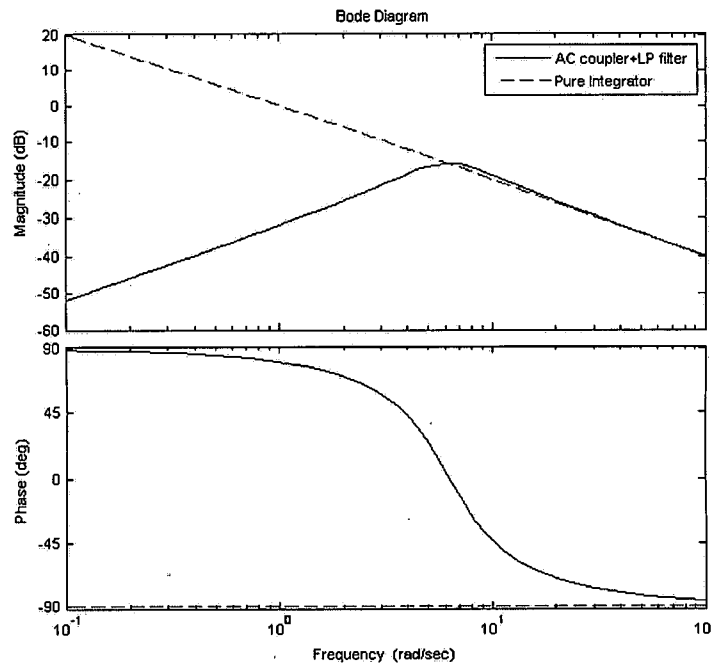


Figure 3-5 Time response of an AC coupler versus a pure integrator



**Figure 3-6 Frequency response of an AC coupler versus a pure integrator**

The low frequency nature of an air-mounted system requires the corner frequency of the AC coupler to be set very low, e.g. 0.1 Hz. This low corner frequency makes the AC coupler to pass very low frequencies with long lasting transients. Note that the similarity of the FRF of an AC coupler with that of a pure integrator is only guaranteed during the steady state response. Considering that an isolation system subject to shocks is almost always in transient response, the use of an AC coupler with low corner frequency, in place of a pure integrator is not advisable.

### III.1.3. Kinematic Kalman Filter

Considering that acceleration integration and displacement differentiation could not give a reliable velocity for the proposed active control system the use of kinematic Kalman filter for the estimation of velocity was considered.

A dynamic Kalman filter uses available measurements of states and/or outputs along with the dynamics of the system and estimates the states that are not measured. Performance of a Kalman filter depends on having sufficient information about the system and noises from the environment and measurement devices. For more details see [8]. Using a dynamic Kalman filter as indicated above requires information about the damping, stiffness and mass (making up the dynamics) of the system. Frequently such information may not be available or may change over time. On the other hand, having a control scheme which can constantly measure or calculate these parameters in real-time requires expensive control hardware. Fortunately, if displacement and acceleration measurements are available one can estimate velocity via Kalman filtering without the knowledge of the dynamics of the system. The estimator providing such a velocity estimate is known as a kinematic Kalman filter [8].

Figure 3-7 shows a block diagram of a kinematic Kalman filter. The input is acceleration, which is easy to measure using piezoelectric or other kinds of accelerometers.

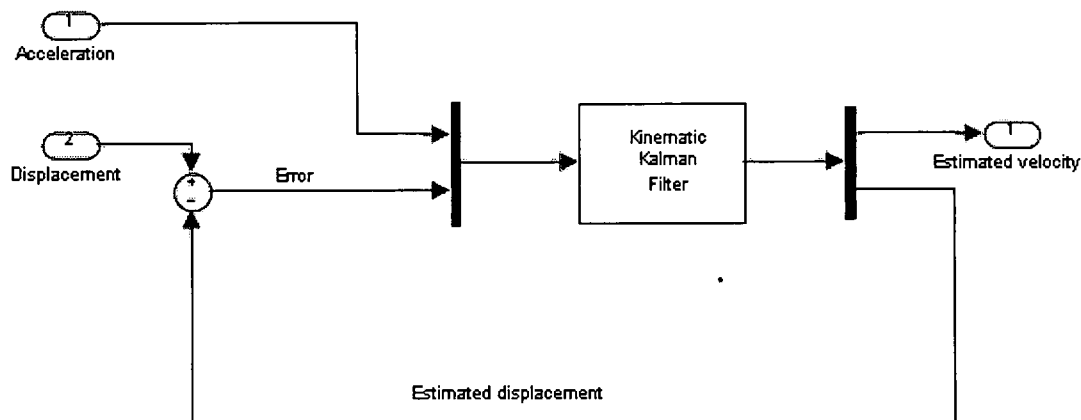


Figure 3-7 Block diagram of a kinematic Kalman estimator.

A displacement sensor is used to measure the height of the system as a measured output to the filter. Outputs of the kinematic Kalman filter are the estimates of velocity and displacement. Estimation error is calculated by comparing the measured displacement signal with the estimated displacement.

The state-space matrices of the system with acceleration as the input and displacement as the output are of the form:

$$A = \begin{bmatrix} 0 & 1 \\ 0 & 0 \end{bmatrix} ; B = \begin{bmatrix} 0 \\ 1 \end{bmatrix} ; C = \begin{bmatrix} 1 & 0 \end{bmatrix} ; D = \begin{bmatrix} 0 \\ 0 \end{bmatrix}$$

The state-space equations are of the form:

$$\begin{bmatrix} \dot{x}_1 \\ \dot{x}_2 \end{bmatrix} = A \begin{bmatrix} x_1 \\ x_2 \end{bmatrix} + B \begin{bmatrix} u_1 \\ u_2 \end{bmatrix}$$

$$\begin{bmatrix} y_1 \\ y_2 \end{bmatrix} = C \begin{bmatrix} x_1 \\ x_2 \end{bmatrix} + D \begin{bmatrix} u_1 \\ u_2 \end{bmatrix}$$

Having L, the Kalman filter gain, the estimator state space matrices are of the form:

$$A_e = \begin{bmatrix} 0 & 1 \\ 0 & 0 \end{bmatrix} ; B_e = \begin{bmatrix} B & L \end{bmatrix} ; C_e = \begin{bmatrix} 1 & 0 \\ 0 & 1 \end{bmatrix} ; D_e = \begin{bmatrix} 0 & 0 \\ 0 & 0 \end{bmatrix}$$

L and B matrices are combined into one matrix ( $B_e$ ) to have the same set of inputs as depicted in Figure3-7. As can be seen, the simplicity of the state-space matrices lowers the mathematical burden of such a filter compared to that of a dynamic Kalman filter and makes it more suitable for real-time computations. Besides, the fidelity of estimation is not at the risk of the modeling inaccuracies.

### **III.2. Analytical Approach**

In this section, an analytical approach for the proposed active control scheme is presented. The goal is to simulate a one-degree-of-freedom air-mounted system under feedback control.

The first part of the approach was the servo-valve simulation. Its transfer functions were identified using experimental frequency response functions for various input voltage amplitudes (resulting in various spool motion amplitudes).

Second order transfer functions were fit to the measured frequency response plots with a small error in the frequency range of interest. The air-mounted system is simulated as a second order spring-mass-dashpot system. The stiffness is inversely proportional to the compliance of the air and directly proportional to the structural stiffness of the air spring derived from the finite element model in Chapter 2.

Finally the feedback control scheme was simulated. Although there are several types of nonlinearities in the system that make the simulation complex, the system represented expected dynamic properties.

### III.2.1. Valve Simulation

The most important part of the simulation process in this section was the servo-valve. To start, a transfer function that resembled the servo-valve's performance in the operating frequency range was determined. An experiment was conducted to find the experimental frequency response of the servo-valve. This experimental frequency response was fit with a second order transfer function which could cover the operating range of frequency.

The experiment set-up included a rigid cylinder (which had zero volume change due to any pressure change) with an air input connected to the valve. The valve in turn was attached to a constant pressure supply. Several tests were conducted for several supply pressures and input voltages to the valve. The corresponding experimental frequency response were plotted and compared with each other. These experiments revealed that the most important parameter in the valve performance was the input voltage. Furthermore, it was observed that the valve performance improved by increasing this voltage.

Figures 3-8 to 3-10 show frequency responses of the valve for input voltages of 1, 2 and 3 ( $V_{ppk}$ ), respectively, and different air spring pressures. From these plots it was inferred that the response of the valve can be approximated by a second

order system with the transfer function of:  $\frac{\omega_n^2}{s^2 + 2\zeta\omega_n s + \omega_n^2}$ . Lack of magnification in the measured frequency response functions (FRFs) indicates that the servo-

valve is not underdamped. This and the shape of the shape of the FRFs resulted in the choice of  $\zeta$ ; in general,  $\zeta$  is measured as the frequency corresponding to the -90 deg phase shift on the phase plot of the experimental frequency response function.

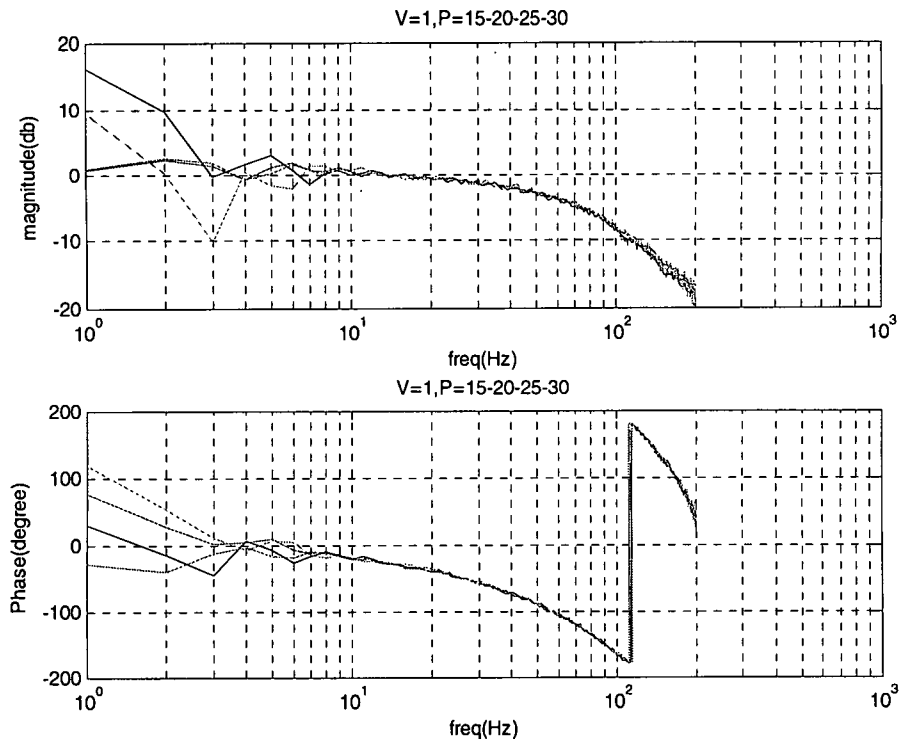


**Figure 3-8 Experimental frequency response of the valve for input voltage of 1 (vppk) for different mount pressures**



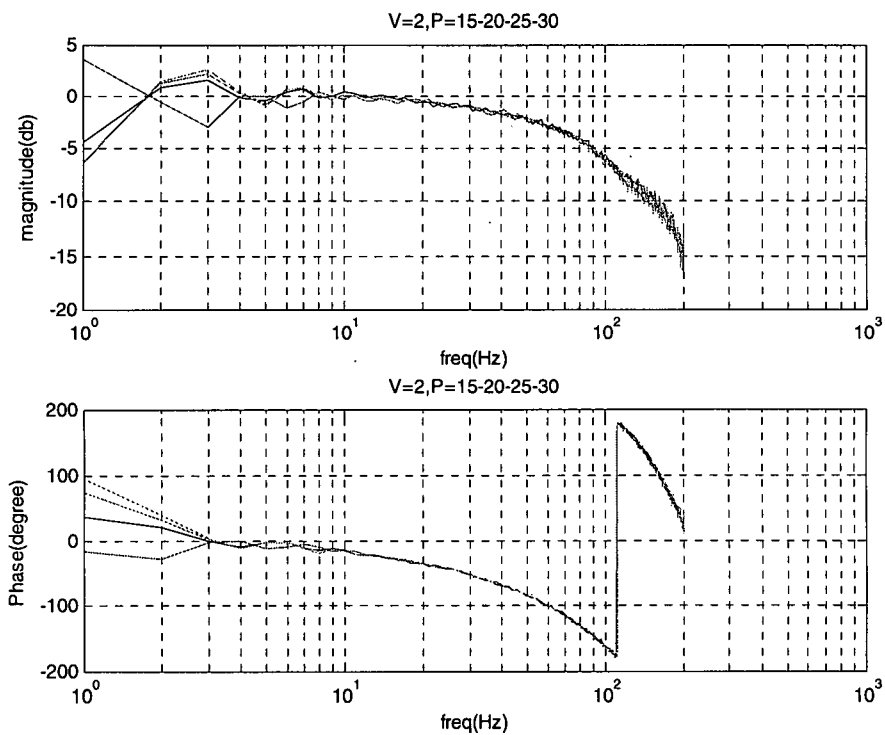


**Figure 3-9 Experimental frequency response of the valve for input voltage of 2 (vpk) for different mount pressures**

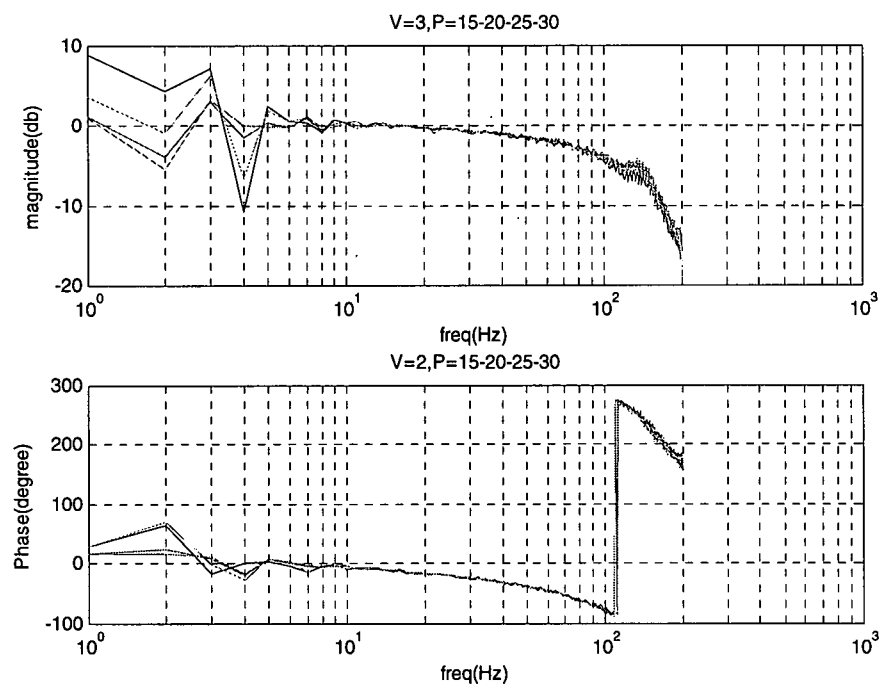


**Figure 3-10 Experimental frequency response of the valve for input voltage of 3 (vpk) for different mount pressures**

This method is useful with ideally fast computer processors where the sampling frequencies are in the order of more than one Gigahertz. Unfortunately, sampling times of the main control board, the internal control board in the valve, and the data acquisition machine were not fast enough to neglect their cumulative delay. Therefore, a transport delay was taken into account to address sampling delay issue. This delay caused the apparent resonance frequency of the system in the phase plot to be lower than what was expected at -90 degrees of phase. Hence, finding the resonance frequency had a degree of trial and error associated with it. This degree was lessened by considering the fact that the real resonance frequency is always higher than it appears in the experimental phase plot (due to the transport delay). However, the resonance frequency at -90 degrees of the experimental phase plot was a good starting point for the approximation. By gradually increasing this frequency, a good fit on the magnitude plot was attained.

Transport delay can be approximated as a linear function of frequency (see figure 4-2) and can be found using the equation below:

$$D_t = 360 f T_t$$

where  $D_t$  is the phase lag caused by sampling delay in degrees,  $T_t$  is the sampling period in seconds, and  $f$  is the frequency of interest in Hz. The sampling delay can be approximated as half of the sampling period. The corresponding phase lag is the difference between the analytical and experimental phases at a certain frequency. Since this kind of delay is almost constant during the sampling process, determining  $D_t$  by comparison is very easy and can be done at any frequency. This delay period was calculated and included in the servo-valve model. Note that if  $TF$  is the transfer function of the valve, the new transfer function with the transport delay is of the form:  $TF_{new} = (TF_{old})e^{T_t t}$  where  $t$  is the time in seconds and  $T_t$  is the sampling delay. Figures 3-11 to 3-14 depict the frequency responses of the approximated transfer functions of the valve for 1, 2 and 3 volts of input voltage to the valve over the corresponding experimental data. The transport delay is also included in

the phase plots (utilizing the formulas above) to match the experimental data. These transfer functions show very good agreement with the experimental data up to more than 100 Hz.

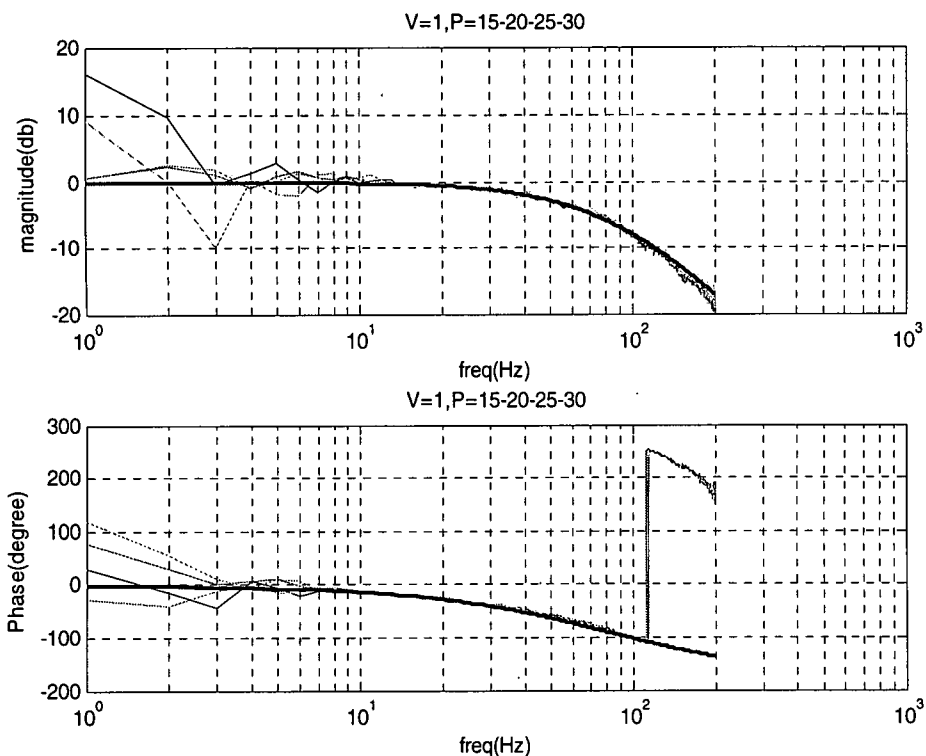


**Figure 3-11 Experimental frequency response versus analytical response (blue thick line) of the valve for input voltage of 1 (vppk) and different mount pressures**

]

However, the difference of frequency response plots depicted in the figures 3-11 to 3-13 are not significant, when the input voltage to the valve is 1 v<sub>ppk</sub>, the valve covers the lowest frequency range (up to 20 Hz), before it affects the phase of the system, among all other voltage inputs. It indicates that the valve has the poorest performance at the voltage input of 1. Hence, to have a reliable transfer function for the valve, the transfer function associated with the input voltage of one was chosen to be included in the valve simulation.

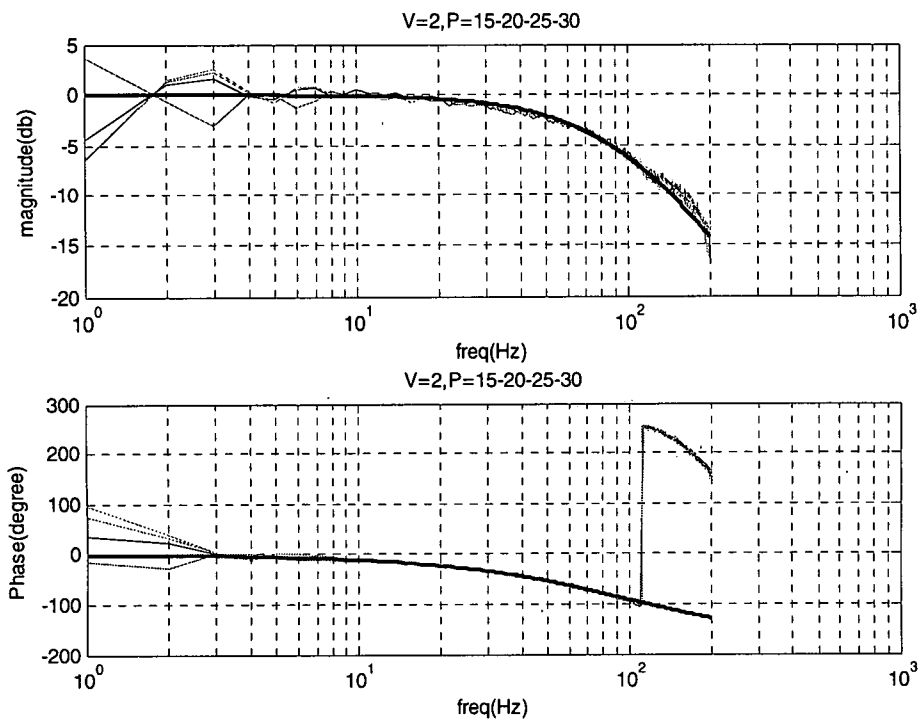


**Figure 3-12 - Experimental frequency response versus analytical response (blue thick line) of the valve for input voltage of 2 (vpk) and different mount pressures**

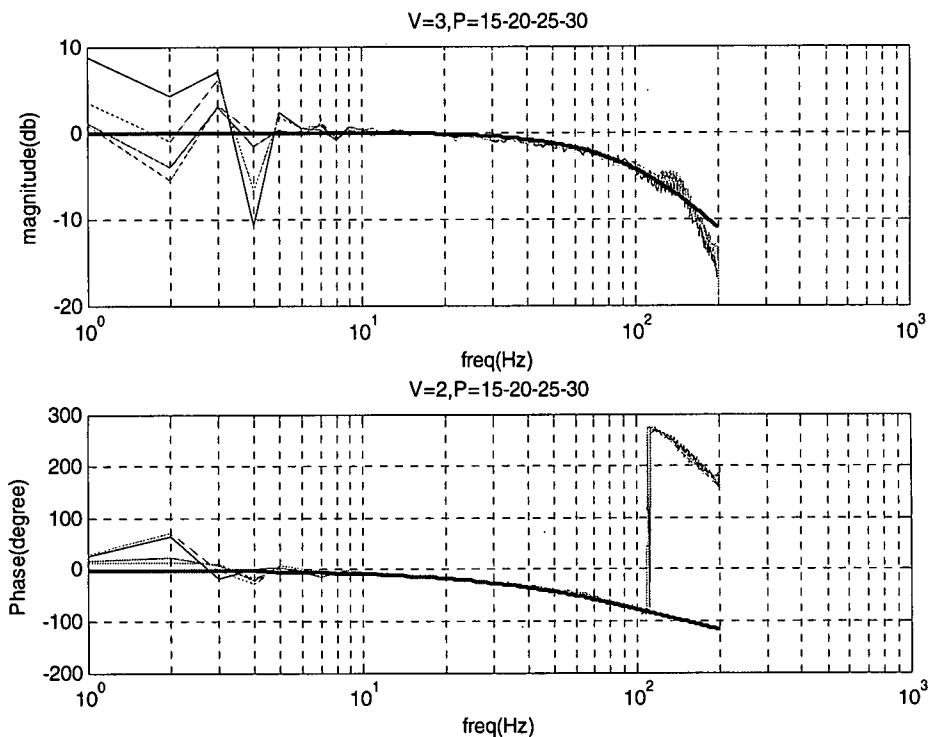


**Figure 3-13 - Experimental frequency response versus analytical response (blue thick line) of the valve for input voltage of 3 (vpk) and different mount pressures**

Figure3-15 shows the final simulation of the servo-valve. Inputs to the valve are the voltage from the control board, the air spring pressure, and the supply pressure. The transport delay and leakage of the valve were also included in the model. Since air is compressible, the nominal flow needs to be calculated to compare the flow at different pressures. In other words, the control flow needs to be calculated at nominal conditions (atmospheric pressure) prior to being sent to the air spring. This flow is scaled again to the internal air spring pressure. In addition, the conversion from voltage (representing the stroke of the spool) to the actual spool position is built into the  $C_v$  block. These factors along with the transfer function play the most important role in the performance of the servo-valve in different pressures and voltages. For the operating range of pressure in our system, flow is approximately proportional to the velocity.

For a narrow orifice, in turbulent flow (Reynolds number larger than 20 for a sharp edge orifice like that of the servo-valve), velocity is determined by:

$$v = C_p \sqrt{\frac{2\Delta P}{\rho}} \quad \text{Eq 3-1}$$

where  $C_p$  is the constant discharge coefficient. This formula was used to calculate the velocity of the output flow from the output port and of the leakage of the valve.

To find the output flow discharge coefficient, a number of experiments were conducted with the same set-up mentioned at the beginning of this section. For each of these experiments, a constant voltage was sent to the valve to build the internal pressure in the rigid reservoir. The pressure was monitored during each experiment and was compared with its corresponding simulation. According to the pressure change in the experiment, the  $C_v$  gain in the simulation that represented the discharge factor  $C_p$  in Eq 3-1 and the cumulative friction of the servo-valve's mechanical parts was modified. These experiments were carried out for different input voltages with different frequencies and magnitudes. Figure3-14 shows the experimental pressure change in the rigid reservoir versus the same pressure change in the simulation after modifying the  $C_v$  gain in the simulation for a voltage of 1 and frequency of 1Hz.

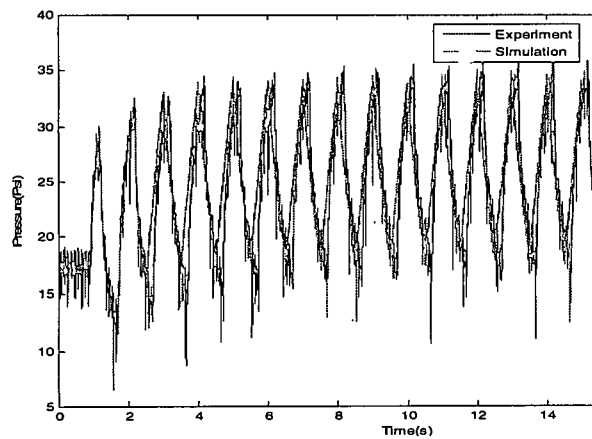


**Figure 3-14 Output pressure change of the valve for input voltage of 1 (vppk) and frequency of 1 (Hz)**

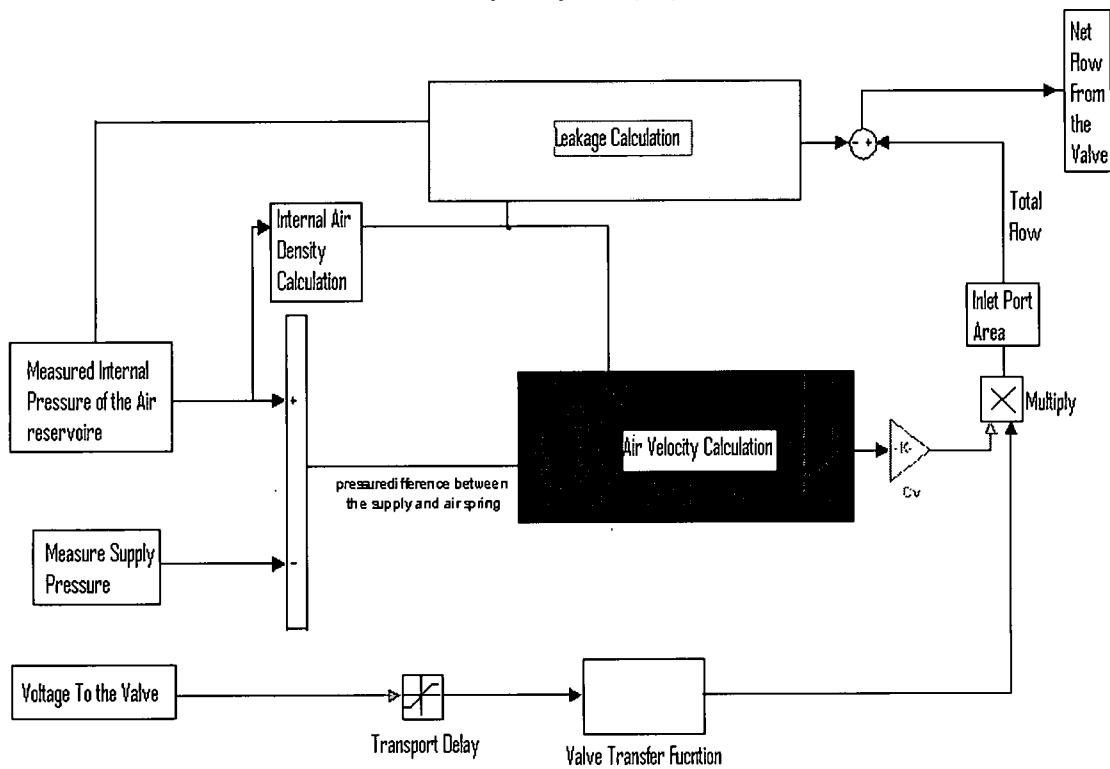


**Figure 3-15 Servo-valve simulation**

### **III.3. One Degree of Freedom (1-DOF) Air-mounted System Simulation**

The simulation of a 1-DOF air-mounted system with the proposed control scheme in section 3 is represented in this section. This simulation includes the servo-valve connected to an air spring suspending the mounted mass. The air-mounted system was simulated as a simple spring-mass-dashpot system. The dashpot represents the damping of the system which is usually less than 2 percent. The spring represents stiffness of the system which includes the stiffness of the air spring's rubber bellows and the inverse of the internal air compliance. These properties were found using the formulas mentioned in Chapter 2.

Figure 3-16 shows a block diagram of the simulation. All the feedback loops affect the flow from the valve to the air spring. The small rectangular summation block indicates that a part of the total flow from the valve is used to build the static pressure (height) of the air spring. Therefore, this amount of flow is subtracted from the total flow to the valve in order to give the dynamic flow. The feedback loops change this dynamic flow in real-time which in turn affect the dynamic properties of the system. This flow becomes dynamic pressure of the air spring by the air spring integration block ( $\frac{1}{s}$ ), and after being multiplied by the air spring cross-sectional area (mount area), it becomes a dynamic force. This dynamic force is fed back to the air-mounted system along with the structural stiffness and the damping force.

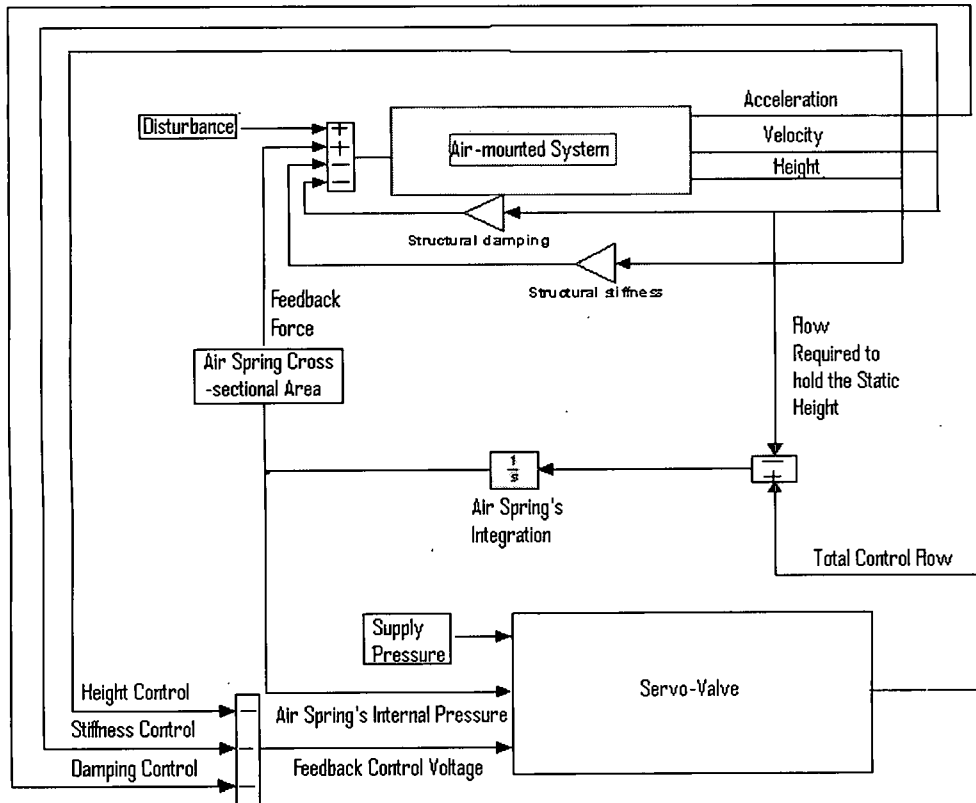


Figure 3-16 1-DOF air-mounted system simulation.

### III.3.1. Results

The simulation showed a very good agreement with the expectations from the control scheme. Figure 3-17 depicts the acceleration of the air-mounted system. As shown, the frequency changes from 5 Hz for a velocity positive feedback, to 7.5 for a negative velocity feedback with almost no change in the damping of the system. Therefore, this control scheme was able to change the stiffness of our system about 125%.



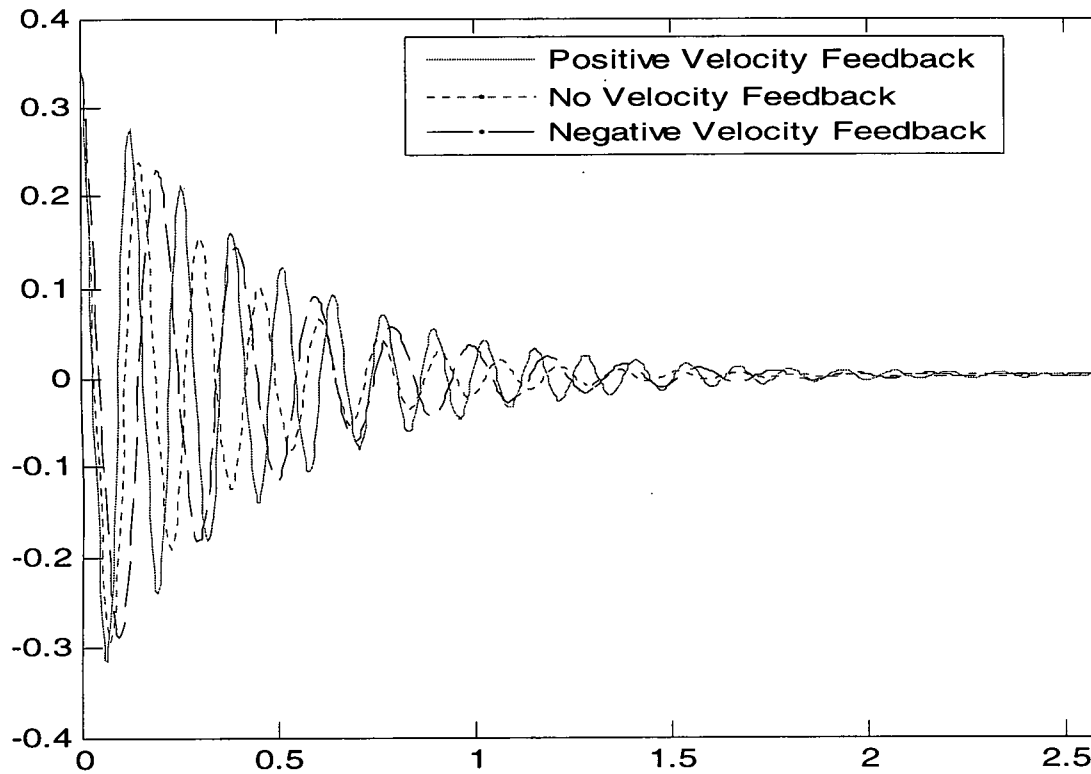


Figure 3-17 Time response of the system to a shock input with different velocity feedbacks

#### III.4. Active Control Scheme

After the properties of the air-mounted system were analyzed, the active feedback control scheme was designed. Figure 3-18 shows a block diagram of the control scheme. In this scheme the controller receives measurements of the acceleration and displacement of the air-mounted system. The acceleration signal is passed through a first order AC-coupler to remove its DC offset and then goes into the kinematic Kalman estimator as the input. This AC-coupled acceleration signal is also implemented in a feedback loop to control the damping of the system in real-time. In addition to the velocity and acceleration feedback loops, a height feedback control loop is also utilized. That is basically a proportional displacement feedback control which uses the low-passed filtered

displacement measured by the sensor as the controlled output. There is also a DC offset added to the summation of the feedback signals which retains the position of the servo-valve's spool. This DC offset sets the spool in the middle position (where the valve is closed) when there are no other signals going to the valve.

The summation of all feedback signals (height control, velocity, acceleration, and DC offset) goes to the control board and becomes a voltage to the servo-valve. Magnitude and sign of this voltage signal control the movement of the spool from its middle position. This in turn lets some air in or out of the air spring.

In this scheme, stiffness and damping can be controlled by modifying proportional gains of velocity and acceleration respectively. Additionally, increasing the height control's proportional gain improves the height control in terms of minimizing the system's reaction time to a change in height due to a disturbance input.

#### III.4.1. Results

In this section the frequency response of the actively controlled air-mounted system is presented. The experiments were conducted on both types of air springs (pneumatic and convoluted). The results showed very good agreement with the simulation and the control scheme were able to increase the stiffness up to at least 125 percent reliably.

Figure 3-19 shows frequency response of the system with a pneumatic mount. Supply pressure was 70 Psi. This figure shows 125 percent change in the stiffness of the system.

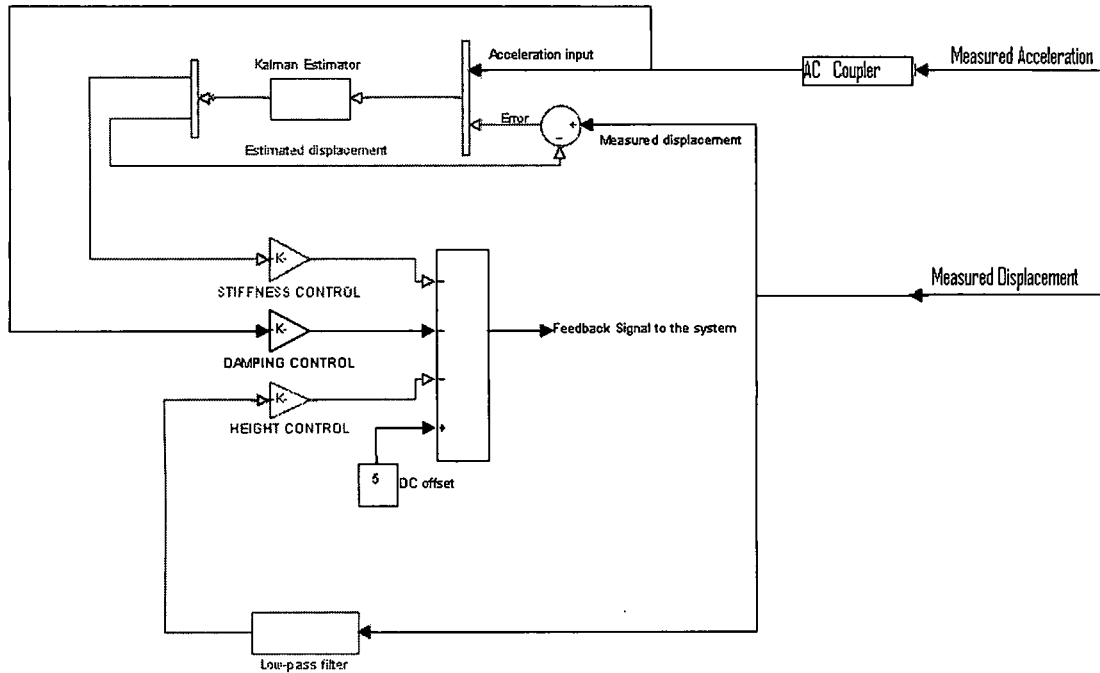


Figure 3-18 The active control scheme.

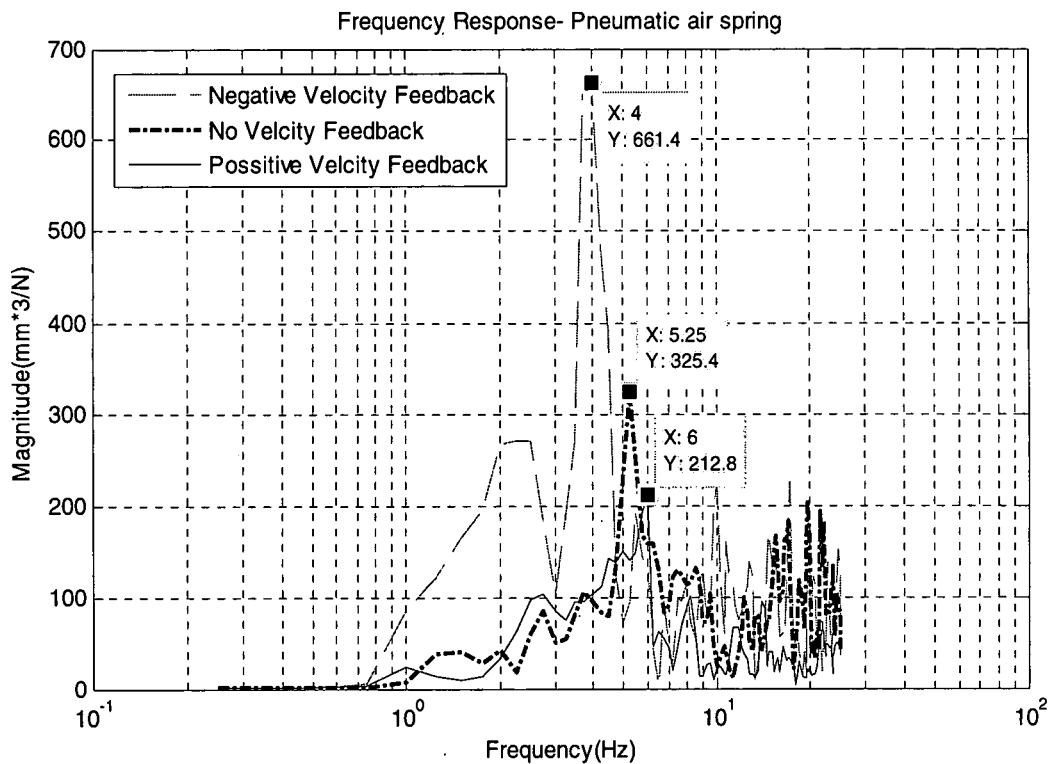


Figure 3-19 FRF of the air-mounted system with a pneumatic air spring

Figure 3-20 shows the frequency response of the same system with a different mounted mass and a convoluted air mount. The results showed 300 percent change in stiffness of the system.

These experiments showed that for the convoluted air spring type the stiffness change is much higher than the pneumatic air spring. This result was predictable due to design of the convoluted air spring. The air inlet in the convoluted type was about twice of the pneumatic type and was located in the bottom metal plate of the air spring. Therefore, the incoming air could easily and equally be disputed in the air spring in a small period of time. Whereas the air inlet in the pneumatic air spring was located on the side of air spring. As a result, the incoming flow could not equally affect the dynamics of the air spring in a short period of time in comparison with the convoluted type.

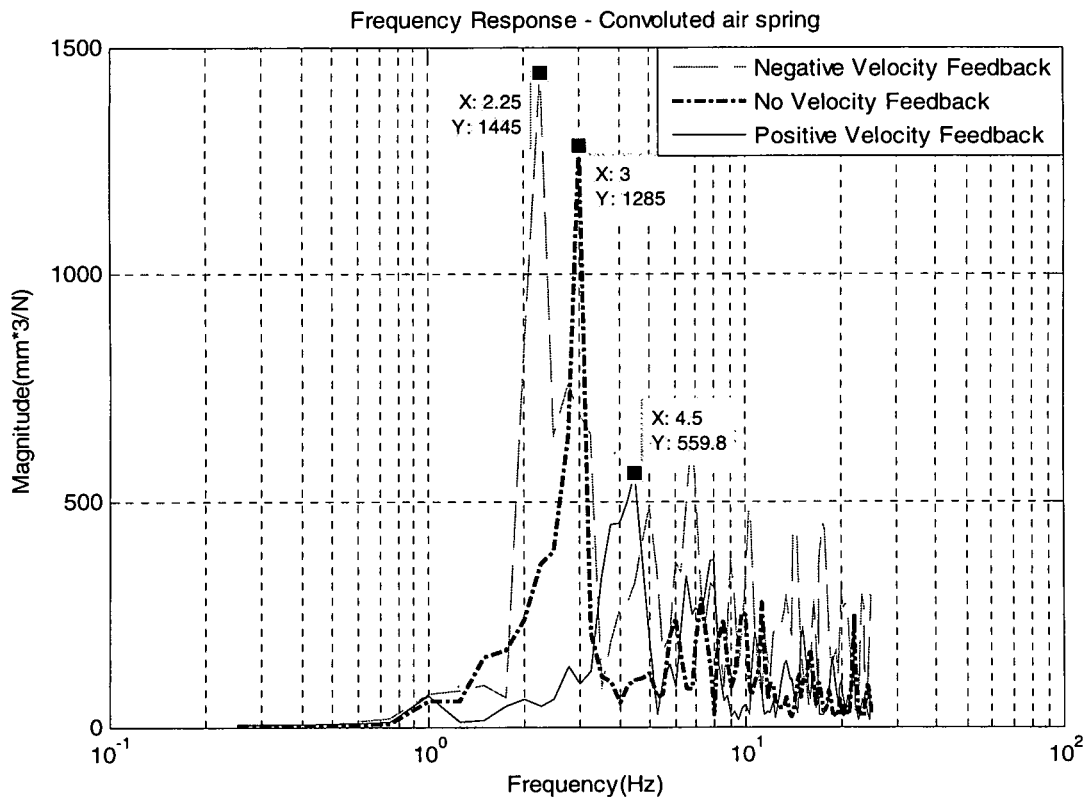


Figure 3-20 FRF of the air-mounted system with a convoluted air spring

## **Summery and Recommendations**

In this thesis two control approaches where studied for stiffness control of air-mounted systems. Both approaches were proved to be valid by using computer simulations and/or experimental results.

First, a semi-active approach was studied using finite element analysis. Basis of the approach was to decrease the volume of the enclosed air in the air spring of the isolation system which in return was changed the stiffness of the system. Results of the analyses in comparison with the available analytical approach showed the validity of the method. Since the semi-active approach could only result in non-continuous stiffness change in the system, to have a continuous stiffness change, an active approach was also proposed. This approach was based on a feedback control scheme with velocity, acceleration, and height feedbacks. The control scheme was primarily validated by a computer simulation of a 1-DOF air-mounted system and later, by a real 1-DOF air-mounted system in the lab. The results showed considerable change in stiffness of the system from 125 percent to 300 percent for the specific set-up used.

Sizes of the active and semi-active set-ups are suitable for many applications especially for isolation of heavy mobile equipment and machinery. The semi-active set-up only needs a water pump with a rather small water reservoir to send the water into or out of the air springs whenever needed (about 1/5 of a liter for each air spring). The active control set-up includes a servo-valve, a control board and a pressure supply. For the active set-up that was experimented in this research an air supply of 70 Psi was used which does not exceed more than 50 lb in weight. However, size of the air supply depends on the desirable performance of the system which varies for different applications. Furthermore, in many cases, passive air isolators are being commonly used

along with regular control valves that maintain their internal pressure with a height or pressure controller. To use the proposed active isolation system in these applications, one needs to change the control valve with a servo-valve. Accordingly, the only additional cost is the price difference between a regular control valve and a servo-valve.

In the active control approach, the accuracy of each controlling parameter (stiffness, damping, and height) is tuned by their associated proportional gains. Since the active control scheme only affects the flow to the air spring via the valve to control all these parameters, not all of these parameters can be completely controlled. In other words, increasing the accuracy of each controlling parameter is usually at the expense of lessening the control of other parameters. Therefore, depending on what the main control goal is more desirable in a specific isolation system, the control scheme's proportional gains should be customized.

In addition, the finite element analysis in chapter II requires more stress-strain data to better model the behavior of the rubber portion of the air spring. The only data available to us was the compression test data provided by the manufacturer which was not adequate. The minimum test data for such a model should include uniaxial and biaxial test data in compression and tension. In addition, the semi-active approach is better to become validated experimentally to assure its functionality.

Achieving more accurate experimental data for the active approach requires using a shaker which was not available for the size of our set-up. Therefore, most of the tests were shock tests with a calibrated hammer. Additionally, a vacuum can be connected to the exhaust of the air exhaust of the servo-valve to have more pressure difference between the pressure supply and the exhaust which hypothetically should result in better stiffness control and faster reaction to shock inputs.

## **Future works**

The control schemes presented in this thesis were able to separately control the stiffness and damping of an air-mounted system. It was shown that the stiffness can increase at least 125 percent with either type of air springs used. However, to have enough control on these parameters, the system need to be calibrated based on the pressure supply, the accuracy of the height controller, amount of the mounted mass, etc. Furthermore, the location of the air inlet and its cross-sectional area should be modified in the pneumatic air spring type to give the best effectiveness in compare with the convoluted type.

In this work a 1-DOF air-mounted system was simulated and tested. We are currently working on a six-degree-of-freedom (6-DOF) system. Such a system has separate air springs with separate servo-valves to study the coupling between the multiple isolators acting on one subject of isolation. In addition, a 6-DOF air-mounted system is planned to be tested to compare its behavior with the simulation. In such a system each air spring is attached to a separate servo-valve and works independently of other air springs. Additionally, the moment of inertia of the mounted mass, which was ignored in the 1-DOF system described in this thesis, will be taken into account.

In both approaches, the dynamics of the system were controlled manually which is not desirable in general. Allowing the user to control these properties may easily result in instability of the system. Therefore, the final design of these approaches should include active detection of dynamics of the system in order to automatically take the necessary action to achieve the desired system's performance

## References

- [1] Dale W. Schubert, "Dynamic Characteristics of a Pneumatic-Elastomeric Shock and Vibration Isolator for Heavy Machinery" Barry Division of Barry Wright Corporation Watertown, Massachusetts. Proceedings of Institute of Environmental Sciences
- [2] Gajarsky, M. "Some Properties of Electro-pneumatic Active vibration Control Systems". *Strojnisky casopis* 35(1-2) (1984), pp.51-65
- [3] I. Hostens, K. Deprez, H Ramon, "An improved design of air suspension for seats of mobile agricultural machines", *Journal of Sound and Vibration* 276 (2004) 141-156
- [4] Agnew, B, "Comparison of approximate forms of air spring shells", *Proceedings of the institution of mechanical engineering science*, Volume 208, Issue 3, 1994, p 207-210
- [5] G.J Stein, I. Ballo, "Active control system for the driver's seat for off-road vehicle", *Vehicle, system Dynamics*, 20 (1991), pp57-78
- [6] G.J Stein, "New results on an electro-pneumatic active seat suspension system", *Proceeding of institution of mechanical engineers*, Vol 214 Part D, 1999
- [7] P. Luque and D.A Mantaras, " Pneumatic suspension in semi-trailers: Part I General considerations and simplified models", *Heavy vehicle systems*, A Special Issue of the *Int. J. of vehicle Design*, Vol. 10, No. 4, pp. 295-308
- [8] Lee D-J., Tomizuka, M., "State/Parameter/ Disturbance Estimation with an Accelerometer in Precision Motion Control of a Linear Motor," *Proceedings of 2001 ASME International Mechanical Engineering Congress and Exposition*, IMECE2001/DSC-24578, 2001
- [9] Eugene, I, Rivin, "Passive Vibration Isolation", Publisher: ASME press, 2003, ISBN 079180187X
- [10] ABAQUS 6.7-1 Documentation.



R002 S93374

## **Vita**

April 6, 1980 Born-Tehran, Iran

2003                      B.S., Khajeh Nasir Toosi University of Technology,  
Tehran, Iran

2006                      Research Fellow, University of Dayton, Dayton, OH,  
U.S.A

2007                      Research Fellow, University of Dayton, Dayton, OH,  
U.S.A

2007                      M.S., University of Dayton, Dayton, OH, U.S.A

### **Field of Study**

Major Field: Mechanical Engineering

Area of Concentration: Solids Mechanics, Dynamic Systems and Control

B.S thesis: "Design and manufacture of a control valve for fine powders' passage", Advisor: Dr. M. Mohammadi-Shojae, Khajeh Nasir Toosi University of Technology, Tehran, Iran, 2003